CRUSTAL STRESSES AND SEISMOTECTONICS IN EASTERN CANADA

Henry S. Hasegawa and John Adams

Earth Physics Branch

Energy, Mines and Resources Canada

Ottawa, Canada, K1A 0Y3

Earth Physics Branch Open File Number, 81-12

Ottawa, Canada, 1981

42 pp. and 19 Figures

Price/Prix: $18.00

TABLE OF CONTENTS

ABSTRACT

Prominent features of the stress field in eastern Canada are discussed with respect to the seismotectonic environment and possible causes of, or major contributors to, the stress field. A ubiquitous feature of the stress field in this region is that the maximum horizontal stress component is larger than the vertical within the top few kilometres of the crust. Fault-plane solutions of shield earthquakes indicate this trend extends to mid-crustal depths. Although the deviatoric (horizontal) stress component within the top few kilometres of the Canadian Shield is well documented, uncertainty exists as to whether deviatoric stress at mid-crustal depths is of the order of a few tens of MPa or a few hundreds of MPa. However, a lower limit of the order of 5 MPa, is inferred from the stress drop of two earthquakes. The azimuth of the deviatoric compression vector, as derived from fault-plane solutions of eastern Canada earthquakes, shows a much greater scatter than the uniform direction (ENE) indicated by northeastern United States earthquakes. However, because of the inherent uncertainty in inferring principal stress directions from deviatoric stress orientations, the question as to whether or not there is uniformity in direction of the maximum principal stress component at mid-crustal depth is still unresolved. More fault-plane solutions of eastern Canada earthquakes are required to resolve this uncertainty. A similar situation exists for _in situ_ stress measurements in eastern Canada. On a broad-scale or regional basis, near-surface stress determinations do not indicate a uniform or general trend but show an appreciable scatter, much of which is likely due to varying local stresses predominating over regional (e.g. plate tectonic) stresses. For certain localized areas, however, stress determinations may be indicating a more uniform pattern; _in situ_ stress measurements north of Lake Superior and Lake Huron can be interpreted as indicating an east-west trend with a scatter of $\pm 45°$. High horizontal stresses may be caused by one or more of the following: erosion; postglacial heating; residual stress from each glaciation - deglaciation cycle; differential postglacial uplift; and plate-tectonic movements. Stress concentration within or surrounding intrusions are induced by density and elastic parameter contrasts between intrusion and host rock. A search for and documentation of, surface evidence of differential postglacial uplift and monitoring of vertical crustal movements is vital to understanding these inherited and cyclic stresses.

As a step towards understanding earthquake prediction in intraplate environments, the Charlevoix region - the most active in eastern Canada - has been selected for continuing physical measurements of processes related to earthquakes. A wide variety of experiments have been carried out; explosion studies to detect changes in P-wave velocities; variations in the magnetotelluric and gravity fields; and variations in ground deformation. Compilation of continuing measurements should enhance our understanding of the seismotectonic environment in eastern Canada.

RÉSUMÉ

Les auteurs se penchent sur les principales caractéristiques du champ de contraintes de l'Est du Canada, sur son environnement sismotectonique et sur les facteurs qui en sont responsables. On constate que, partout dans la région, la composante horizontale maximale de la contrainte est généralement supérieure à la composante verticale dans les premiers kilomètres d'épaisseur de la croûte. D'après les plans de faille résultant des tremblements de terre du bouclier, cette tendance se maintient jusqu'aux profondeurs moyennes de la croûte. Même si l'on est bien documenté au sujet du déviateur des contraintes (composante horizontale) dans les premiers kilomètres d'épaisseur du Bouclier canadien, on ne sait pas encore avec certitude si le déviateur existant dans les profondeurs moyennes de la croûte est de l'ordre de quelques dizaines ou de quelques centaines de MPa. Toutefois, il ressort de la chute de contraintes liée à deux tremblements de terre que la limite inférieure serait de l'ordre de 5 MPa. L'azimut du déviateur des contraintes, calculé d'après les plans de faille résultant des tremblements de terre de l'Est du Canada, est beaucoup plus variable que la direction, plutôt uniforme, indiquée par les séismes du Nord-Est des Etats-Unis. Cependant, la déduction d'une direction principale à partir de l'orientation du déviateur des contraintes étant entachée d'une certaine incertitude, il n'a pas encore été possible de déterminer s'il y a uniformité dans la direction de la composante principale maximale des contraintes aux profondeurs moyennes de la croûte. Seule l'étude d'autres résolutions de tremblements de terre de l'Est canadien sur des plans de faille permettra de lever cette incertitude. Une situation semblable existe dans le cas des mesures de contraintes effectuées _in situ_ dans l'Est du Canada. A l'échelle d'une région, le calcul des contraintes de la proche surface révèle non pas une direction uniforme ou générale, mais une orientation largement variable, qui est probablement attribuable en grande partie à la prédominance des contraintes locales variables sur les contraintes d'échelle régionale (comme celles qui relèvent de la tectonique des plaques). Dans certaines régions localisées, toutefois, la détermination des contraintes indique peut-être l'existence d'une direction plus uniforme; ainsi, les mesures _in situ_ effectuées au nord du lac Supérieur et du lac Huron peuvent être interprétées comme une indication d'une orientation est-ouest $\pm 45°$. La valeur élevée d'une composante horizontale peut être causée par un ou plusieurs des facteurs suivants: érosion, chauffage post-glaciaire, contraintes résiduelles de chaque cycle de glaciation-déglaciation, soulèvement post-glaciaire différentiel et tectonique des plaques. Une concentration de pressions à l'intérieur ou autour des intrusions est provoquée par les différences de masse volumique et d'élasticité entre la roche intrusive et la roche encaissante. Pour comprendre ces contraintes héritées et cycliques, il est essentiel de trouver et d'expliquer les manifestations en surface d'un soulèvement post-glaciaire différentiel.

Dans le but de comprendre la prévision des séismes dans les milieux intra-plaques, les chercheurs ont choisi la région de Charlevoix, la plus active de l'Est du Canada, pour effectuer des mesures physiques continues sur des processus associés aux tremblements de terre. Déjà, diverses expériences ont été réalisées: études par explosions visant à détecter les variations de la vitesse de l'onde P, variations des champs magnétotelluriques et gravimétriques et variations de la déformation du terrain. L'accumulation des mesures devrait nous permettre de mieux comprendre l'environnement sismotectonique de l'Est du Canada.

INTRODUCTION

In eastern Canada, in situ stress measurements in mines and boreholes, rockbursts in mines, and young folds, faults and pop-ups all indicate a high horizontal component of stress. That is, a stress environment for which the maximum horizontal component of stress is greater than the vertical. Earthquake fault-plane solutions indicate the deviatoric compression vector to have a larger horizontal than vertical component at focal depths ranging from 9-17 km. However the azimuth of maximum principal stress, as inferred from diversified phenomena and measurements, shows an appreciable scatter. An understanding of the primary contributors to the stress field in eastern Canada is an integral and important aspect of the design of stable underground engineering structures, mine safety and the safe disposal of radioactive wastes. The latter topic is receiving an ever-increasing amount of attention in recent publications (e.g. Dence and Scott, 1979; Berry and Hasegawa, 1979; Bird, 1979; Tammemagi, 1979; Price, 1979; Strangway, 1980; Mair and Green, 1981).

Various disciplines are contributing to our knowledge of the seismotectonics and stress field in eastern Canada, and we propose to mention briefly the scope of our review before discussing the results.

The distribution of seismicity in eastern Canada (Leblanc and Buchbinder, 1977; Basham et al., 1979; Stevens, 1980), the spatial correlation of seismicity in western Quebec with geological and geophysical data (Forsyth, 1981), the association of seismicity with tectonic activity in the Charlevoix region (Dunbar and Garland, 1975; Hasegawa and Wetmiller, 1980), and fault-plane solutions of several Canadian Shield earthquakes are providing us with a broader perspective as to why earthquakes tend to occur in clusters or "zones". Fig. 1, which shows the seismicity of southeastern Canada together with tectonic provinces and prominent geological structures, illustrates this tendency for earthquakes to cluster in the region. In situ stress measurements by overcoring (Herget, 1980) and hydrofracturing (Haimson, 1978) are revealing quantitative measures of the stress field at depths to about 2 km.

Contemporary crustal movements (e.g. Frost and Lilly, 1966; Vanicek and Hamilton, 1979; Walcott, 1972; Vanicek, 1976; Lambert and Vanicek, 1979) indicate on-going tectonic processes. A search for, and documentation of, postglacial faults provides us with a more detailed account of the temporal behaviour and spatial distribution of rapid energy release of stored stress during deglaciation (Adams, 1981). Satellite imagery delineates lineaments and faults in seismotectonic regions of interest (e.g. Moore, 1979). A heat-flow history of the Canadian Shield constrains post-tectonic events and parameters such as strength and thickness of crust (Jessop and Lewis, 1978; Taylor and Judge, 1979). In certain regions steep lateral gradients in the gravity anomaly field correlate with seismicity (Basham et al., 1979; Goodacre and Hasegawa, 1980). Geologists are outlining relatively unstable regions from a tectonic viewpoint (e.g. Ermanovics and Card, 1980). A high resolution seismic reflection experiment across a batholith demonstrates that major fracture zones may exist at shallow depths in "homogeneous" batholiths

(Mair and Green, 1981). Phenomena associated with glaciation and deglaciation can generate appreciable flexural stresses (Walcott, 1970; Stein et al., 1979) and shear stresses (Price, 1979). Thus the data and theory from various disciplines are contributing to our understanding of the stress regime, the location of weakened zones, and the seismotectonics of eastern Canada.

A composite description of the variation with depth of the stress field is obtainable from different techniques. Down to depths of several hundreds or a few thousands of metres, in situ stress measurements from overcoring indicate the orientation and magnitude of the three principal stress components. At greater depths, down to several kilometres, hydrofracturing can determine the magnitude and orientation of the principal stresses when both the borehole and one of the principal stress components are vertical or near vertical. At still greater depths, say down to several tens of kilometres, fault-plane solutions of earthquakes indicate the orientation and relative magnitudes of the deviatoric stress components.

This report is intended as a summary of our knowledge of the stress field in eastern Canada. Since major changes in the stress field due to glaciation-deglaciation are relevant, descriptions of certain surficial postglacial phenomena are also presented. The description of the stress field in eastern Canada is preceded by a definition of several basic concepts used in this report, namely deviatoric stress, the Coulomb-Mohr failure criterion and equivalent force representations of earthquake source mechanisms.

DEVIATORIC STRESS

Consider the tetrahedron shown in Fig. 2b. The total resultant stress acting on the inclined surface is represented by $\overline{\sigma}$ and the normal to the plane by $\overline{n}$, which has direction cosines ℓ_1, ℓ_2, ℓ_3. The components of $\overline{\sigma}$ along the co-ordinate axes are (see Fig. 2a).

$$\begin{bmatrix} \sigma_{n1} \\ \sigma_{n2} \\ \sigma_{n3} \end{bmatrix} = \begin{bmatrix} \sigma_{11} & \sigma_{12} & \sigma_{13} \\ \sigma_{21} & \sigma_{22} & \sigma_{23} \\ \sigma_{31} & \sigma_{32} & \sigma_{33} \end{bmatrix} \bullet \begin{bmatrix} \ell_1 \\ \ell_2 \\ \ell_3 \end{bmatrix} \quad ...(1)$$

A modification of Eq. (1) using the associated principal stresses σ_1, σ_2 and σ_3, where $\sigma_1 > \sigma_2 > \sigma_3$, is as follows:

$$\begin{bmatrix} \sigma_{n1} \\ \sigma_{n2} \\ \sigma_{n3} \end{bmatrix} = \begin{bmatrix} \sigma_1 & 0 & 0 \\ 0 & \sigma_2 & 0 \\ 0 & 0 & \sigma_3 \end{bmatrix} \bullet \begin{bmatrix} \ell_1 \\ \ell_2 \\ \ell_3 \end{bmatrix} \quad ...(2)$$

The mean stress, σ_m is defined as $\sigma_m = (\sigma_1 + \sigma_2 + \sigma_3)/3$, the deviatoric stress components are represented by a superscript D, and are $\sigma_1^D = \sigma_1 - \sigma_m$, etc. Therefore Eq.(2) can be rewritten as follows (e.g. see Saada, 1974):

$$\begin{bmatrix} \sigma_{n1} \\ \sigma_{n2} \\ \sigma_{n3} \end{bmatrix} = \left\{ \begin{bmatrix} \sigma_m & 0 & 0 \\ 0 & \sigma_m & 0 \\ 0 & 0 & \sigma_m \end{bmatrix} + \begin{bmatrix} \sigma_1^D & 0 & 0 \\ 0 & \sigma_2^D & 0 \\ 0 & 0 & \sigma_3^D \end{bmatrix} \right\} \bullet \begin{bmatrix} \ell_1 \\ \ell_2 \\ \ell_3 \end{bmatrix} \quad ...(3)$$

In seismotectonics and tectonophysics, the strict mathematical definition of the deviatoric stress component is generally not used. In place of σ_m, as defined above, the mean overburden pressure, σ_v, is used. In most cases $\sigma_v \simeq \bar{\rho}gh$ (i.e. only slight perturbation due to flexural rigidity of crust) where $\bar{\rho}$ is the average overburden density, g the acceleration due to gravity and h, the overall thickness of the overburden (e.g. McGarr and Gay, 1978: Herget, 1980). The mean overburden pressure is often referred to as the lithostatic stress component.

COULOMB-MOHR FAILURE CRITERION

Consider a volume in which weakened zones are oriented in a more-or-less random manner. Let the maximum and minimum principal stress components be represented by σ_1 and σ_3 respectively. For an arbitrary plane oriented at an angle ψ (or normal at angle β) with respect to σ_1 as illustrated in Fig. 3a, the normal stress component is represented by σ_n and the shear stress, by τ. When a critical stress condition (τ_c) occurs, failure generally takes place along a plane for which ψ is of the order of $\pi/6$. For this case the Mohr circle, with radius $(\sigma_1 - \sigma_3)/2$, just touches the Coulomb failure line for which $\tau_c = \tau_o + \mu_f \sigma_n$, where τ_o is the cohesive strength and μ_f, the coefficient of friction, which equals $\tan\phi$. Failure can occur in different ways, such as by a variation in σ_n, a weakening of τ_o, a decrease in μ_f, or a combination of these different modes. Since actual processes of sudden failure can be very complicated (e.g. see Hanks and Raleigh, 1980, for summary) it is not known to what extent the Coulomb-Mohr failure criterion, without some modification, holds for earthquakes at various focal depths. However the unmodified form is generally considered to be applicable to shallow-focus intraplate earthquakes (e.g. see Healy et al., 1968; Raleigh et al., 1972; Sbar and Sykes, 1973, 1977; Pomeroy et al., 1976; N.H. Sleep, personal communication, 1977).

From a statistical treatment of carefully selected in situ stress measurements, most of which are within a kilometre of the surface of the ground, Jamison and Cook (1980) show that the value of τ_o is essentially zero. For this case, whereby the rocks are highly fractured so that frictional strength predominates, Byerlee's law (frictional resistance is represented by a simple bilinear empirical relation over a range of normal stress from about 3 MPa to 1.7 GPa) converted to maximum or minimum stress is a good upper or lower bound, depending on whether the pore pressure is hydrostatic or subhydrostatic (Brace and Kohlstedt, 1980).

EARTHQUAKE FAULT PLANE SOLUTIONS

Equivalent Source Representations

Three equivalent earthquake source representations are shown schematically in Fig. 4. Physically earthquakes are usually associated with sudden slip along a weakened region (Fig. 4a). Equivalent source representations in an unfaulted region are shown in Figs. 4b and 4c. (e.g. see Maruyama, 1963; Burridge and Knopoff, 1964; Hodgson and Stevens, 1964; Aki and Richards, 1980). That is, these three representations generate identical seismic radiation patterns. Note that the equivalent force representations are symmetric with respect to two orthogonal planes, one plane parallel to the actual fault and the other, perpendicular to the actual plane, i.e. parallel to the auxiliary plane. A schematic Mohr representation of the principal stress components is shown in Fig. 4d. For the present discussion it is convenient to set ($\sigma_1 - \sigma_2$) and ($\sigma_2 - \sigma_3$) equal to each other (see Fig. 4d) since we are concerned with equivalent source representations and not the inferred ambient stress field, which could be different (e.g. see Zoback and Zoback, 1980). The Mohr representation for Fig. 4c is shown in Fig. 4e. The deviatoric compression, P, and extension, T, vectors are related to the null vector, which is perpendicular to the plane of the sheet and is represented by a solid dot in Fig. 4c. The Coulomb failure line corresponding to fault-plane solutions is horizontal, as shown in Fig. 3b, and this condition corresponds to the limiting case where the coefficient of friction, μ_f, is zero.

Caution should be exercised when associating the equivalent force representation, i.e. principal axes of the moment tensor (Fig. 4c) with the principal stress axes or ambient stress field. For example if there is only the fault-plane solution of a single earthquake in the region of interest, then the orientation of the maximum horizontal component of the tectonic stress field could vary appreciably (35° - 40°) from the orientation of the deviatoric stress components (e.g. see McKenzie, 1969; Raleigh et al., 1972; Zoback and Zoback, 1980). On the other hand, if a fairly large number of fault-plane solutions within a region have similar oriented deviatoric stress vectors, then they probably lie within a uniform regional stress field (e.g. Sbar and Sykes, 1973; 1977; Zoback and Zoback, 1980).

STRESS REGIME IN EASTERN NORTH AMERICA

Northeastern United States

Fault-plane solutions have been used to complement in situ stress measurements (at shallower depths) so as to infer the direction of the maximum compressive stress component of a tectonic stress field in an intraplate environment (Sbar and Sykes, 1973, 1977; Zoback and Zoback, 1980). Based on the relatively uniform direction of the maximum horizontal component and deviatoric compression of the stress field shown in Fig. 5, Sbar and Sykes inferred that this consistency is probably due to tectonic forces associated with spreading at the mid-Atlantic ridge. Hence local remanent stresses appear to be relatively unimportant in the region. When the fault plane was known from geologic or geophysical evidence near the epicentre, Sbar and Sykes rotated the orientation of the deviatoric compression (P) vector from 45° to 30°, with respect to the fault plane. The effect of this change on the Coulomb-Mohr failure criterion can be seen by comparing Fig. 3b with Fig. 3c; the latter gives a more realistic slope to the Coulomb failure line (see Handin, 1966). Other characteristics of northeastern United States earthquakes are a shallow (less than 15 km) focal depth and a source mechanism that is either a thrust or strike-slip type of faulting (Herrmann, 1979; Yang and Aggarwal, 1981).

Eastern Canada

The behaviour of the stress pattern at depth shows two general trends. Firstly the maximum principal stress tends to be horizontal and greater than the vertical component. Secondly there appears to be an appreciable scatter in the direction (or azimuth) of the maximum principal stress component (for a review see Ranalli and Chandler, 1975; Lindner and Halpern, 1977; Franklin and Hungr, 1978).

Fig. 6 (top graph) depicts the variation with depth of the ratio of maximum horizontal-to-vertical stress component for western Ontario (from Herget, 1980); the locations of these in situ stress measurements are represented by numbers 1-7 in Fig. 7. The relative size of the stress components, as inferred from fault-plane solutions of the larger magnitude, recent eastern Canada earthquakes (see Hashizume, 1974; Horner et al., 1978; Horner et al., 1979; Hasegawa and Wetmiller, 1980), is shown in the lower part of Fig. 6. The amount of separation of the three principal components at mid-crustal depth is not known, i.e., whether the deviatoric stress is in the hundred MPa range (see Hanks and Raleigh, 1980) or in the ten MPa range (e.g. see Weiss, 1977). However the stress drop of two shield earthquakes is 5 MPa, (Horner et al., 1978; Hasegawa and Wetmiller, 1980) which puts a lower limit on the deviatoric stress component at mid-crustal depths.

An azimuthal distribution of the maximum principal stress direction in southeastern Canada, as determined from overcoring, hydrofracturing and earthquake fault-plane solutions are displayed in the lower part of Fig. 7. For the overcoring the solid dots in the smaller circles are equal area net projections of the maximum principal stress components in the lower hemisphere (1-7 from Herget, 1980). The line segments in the smaller circle (8) just north of Lake Ontario represent a stereographic projection of vertical fractures formed during hydrofracturing and indicate the strike of the maximum horizontal stress component (Haimson, 1978). The pair of colinear arrows associated with fault-plane solution of the earthquakes (listed in Table 1) represent the orientation of deviatoric stress vectors, with inward pointing arrows denoting deviatoric compression and outward pointing arrows, extension.

Neither measured nor inferred directions of maximum principal stress in eastern Canada (excluding those in northeastern part) indicate the uniform orientation that is apparent in the northeastern United States (cf. Fig. 5 with Fig. 7). The apparent "scatter" in direction of about $\pm 45°$ from an east-west orientation shown by the overcoring measurements, is considered to be real and is likely due, in some regions, to remanent stresses from previous local tectonic events (no. 1 of Fig. 7), and in other regions to a nearly isotropic horizontal stress field (e.g. no. 5 of Fig. 7, from Herget, 1980).

Locally-induced stresses may be significant or even dominant in certain regions of eastern Canada (e.g. see Herget, 1980; Nyland, 1973; Dunbar and Garland, 1975; Price, 1979). Since uncertainties in stress orientation inferred from fault plane solutions can be $\pm 30°$, firm conclusions cannot be drawn as to whether or not the orientation of the maximum horizontal component of the regional tectonic stress field in eastern Canada is unidirectional at mid-crustal depth. Thus the sparse fault-plane solutions of southeastern Canada earthquakes are not able to rule out the possibility of a uniform stress field at mid-crustal depth in the region.

The apparent bimodal "scatter" or spread in the hydrofracture results (no. 8, Fig. 7) stems from a variation in azimuth of the maximum compressive stress component with depth or layer formation. Measurements in the shallow (75 m - 105 m) Ordovician limestones indicate a maximum stress orientation in the range of 60° - 80° (clockwise from geographic north), with the underlying Precambrian rocks a range of 22° - 27°. Moreover, the data suggest an abrupt discontinuity in stress magnitude near the interface (see Haimson, 1978).

In summary, the results tend to cluster, to a greater extent about an east-west direction than a north-south direction. An exception may be the m_b 4.9, 1973 Quebec-Maine border earthquake. However, this earthquake is also different in not occurring within the shield and may be affected by conditions particular to the northern Appalachian tectonic province; a revised fault-plane solution for this earthquake by Herrmann (1979), who used surface wave data in addition to P-wave first motions, indicates a NNE azimuth for the deviatoric compression vector.

NEAR SURFACE STRESSES AND STRESS DIRECTIONS

Stresses that cause earthquakes or are measured in deep mines also affect the surface rocks, but the identification of their magnitude and direction is less certain because they are affected by the topography of the free surface and by the numerous planes of weakness - joints, cleavages, old faults, bedding planes - that occur there. If suitably oriented planes are available, movement may occur on them rather than on new planes through previously intact rock, and so the deduced stress direction will be influenced by the orientation of the existing plane.

A second problem with the interpretation of the surficial features is that they range considerably in age and older features may have formed in stress environments that differ considerably from each other as well as those of present day. Of particular importance in comparing stress directions from surficial features with those from the adjoining United States is that eastern Canada was almost entirely covered by 2 km of ice less than 14,000 years ago, and that the stresses produced by this crustal loading may have dominated over other ambient stresses near the surface.

Therefore we list and discuss the shallow stress measurements, and those surficial phenomena indicating high horizontal stresses, in order of increasing age so that a distinction can be made between contemporary or historic (<100 years), postglacial (? 8,000 to 14,000 years), and glacial or preglacial (>14,000 years) stresses.

Stress measurements at shallow depths

Direct measurements of horizontal stresses have been made at shallow depths in connection with engineering construction (Table 2A). The measurements were mostly made at depths less than 30 m (in contrast to the deep mine measurements reported by Herget, 1980), and are chiefly in thinly-bedded sedimentary rocks rather than in the massive granites and gneisses of the shield. However, like the deep measurements, the shallow measurements all show horizontal stresses far greater than vertical stresses. In southern Ontario the maximum horizontal stresses near the surface are in the range 3-14 MPa (Lo, 1978) and, in these shallow measurements at least, the stress magnitude is nearly independent of depth. In interbedded siltstones and sandstones, the softer siltstones sometimes appear to be more highly stressed than the harder sandstones, although this difference may be due to the difficulty in measuring the Young's Modulus of soft rocks (Franklin and Hungr, 1978).

There is a considerable variability in the stress orientation shown by the measurements, although an east or northeast trend is weakly supported by the data (Fig. 8). However, as shown by the hydrofracturing measurements at Darlington, Ontario (Haimson, 1978), there may be a sharp discontinuity in stress magnitude and direction at the base of the sedimentary rocks that cover the Canadian Shield, or at other interfaces, and so it is not clear just what the relationship is between the shallow stress measurements and the stress field at depth.

Quarry-floor buckles

When overburden and rock are removed from quarries, heave of flat-lying strata, or of massive rock with horizontal joints, sometimes occurs on the quarry floor (Table 2B). These quarry-floor "buckles" may be 100 m long and rise 1 to 2 m above the quarry floor (Lo, 1978; Saull and Williams, 1974; White et al., 1973). The buckles are caused by high horizontal stresses that are released when the overburden is removed, and in the Marmora Quarry a horizontal stress of 14 MPa was calculated for one buckle by assuming the strata to be a fixed-ended beam (Coates, 1964). The orientation of the buckles tends to be normal to the direction of largest horizontal stress shown by other methods (Sbar and Sykes, 1973), although the proximity to quarry walls and the presence of joints or other planes of weakness in the rock may influence their exact orientation.

An unusual phenomenon similar to quarry-floor buckles and the pop-ups discussed below was the growth of a surface fold in open country near Westover, Ontario, in 1949 (Karrow, 1963). Mainly during one night, bedrock was tilted 20° and lifted to form a 1.3 m high ridge which was 100 to 200 m long and dammed a small stream; trees and a small bridge were lifted vertically. Unlike the quarry-floor buckles which are caused by the removal of rock load, the triggering mechanism of the Westover upheaval is not apparent.

Another feature that indicates contemporary high horizontal stresses is the "squeeze" of slot-shaped excavations such as canals. The phenomenon has been noted especially in power canals near Niagara Falls (Lo, 1978), and calculations indicate horizontal stresses of 3 to 10 MPa at depths of 20 m.

Postglacial faults

Before the glaciers retreated from eastern Canada about 14,000 to 7,000 years ago, they smoothed and striated the bedrock of the region. In many areas this bedrock now shows the effects of postglacial faulting (Adams, 1981). The faults have minute throws (a few tens of mm or less), and are only detected because the surfaces they displace as so smooth. Although the individual fault throws are small, they are systematic and could cumulate to a significant displacement if faulting were as widespread beneath surficial cover as it appears to be on outcrops.

The displacements of the glaciated surfaces occur on bedding-planes, cleavages or joints or other high-angle pre-existing planes of weakness. Where the dip of the plane can be observed, the faulting is always reverse (thrust) and so the postglacial faults appear to represent compression normal to the azimuth of the fault.

Figure 9 shows the location of known postglacial faults as taken from Adams (1981) and from the hitherto unpublished observations in Table 2C. Faults have been observed in four regions - Nova Scotia-New Brunswick; Eastern Townships, Quebec; Ontario-Quebec border, and western Ontario - but need not be limited to these regions. If interpreted as modern thrust faults, the faults in the eastern two regions indicate southeast-northwest compression, (Fig. 9) and those in the western two regions north-south compression (Figs. 9 and 10c), in contrast to the generally considered east or northeast compression in northeastern United States (Sbar and Sykes, 1973).

However, the orientation of the faults is more consistent with the direction in which the ice retreated, since the faults are roughly ($\pm$ 20°) parallel to the ice margins mapped by Prest (1970). On this basis the faults may reflect a transient unloading response to deglaciation that occurred on those pre-existing planes of weakness which had a suitable orientation.

Pop-ups

"Pop-ups" are postglacial surficial folds that indicate the orientation of horizontal compression (Table 2D) as do the buckles in quarries (Lo, 1978). A typical pop-up is an anticlinal ridge of broken rocks 5 to 10 m wide, 50 to 500 m long, and with flank dips of about 20° that may rise 1 to 2 m above the level of the surrounding ground. Pop-ups probably form because the bedded nature of the flat-lying sedimentary rocks allows the decoupling of the topmost 1 to 2 m along some bedding plane or shale layer, and because the horizontal stress of 5 to 10 MPa then exceeds the crushing strength of the rock beam.

Because of their narrowness, and their similarity to quarry floor buckles which are only a few metres thick, it is unlikely that the anticlinal disturbances extend to any great depth. However, some authors have suggested that the pop-ups may be the surface expression of faults (see examples cited by Adams, 1981, p. 13), and as none has been excavated, the deep structure of the pop-ups remains uncertain.

On some pop-ups, glacial striae can be traced across the axis of the fold, and the topographic expression of the pop-ups shows that they postdate ice retreat, as ice moving across the feature would remove the broken rock and truncate the fold. Only six pop-ups from the literature are definitely postglacial and have documented orientations (Table 2D): They indicate north-south compression (Figure 9), but like other features show a large scatter about the preferred direction (Figure 10).

The pop-ups all occur within the Paleozoic sedimentary cover of southern Ontario, and none has been found on the Precambrian Shield itself, perhaps for three reasons. Firstly, the shield rocks are stronger than the Paleozoic sediments, and their crushing strength might not be exceeded at the surface. Secondly, while the shield rocks have horizontal sheeting-joints (and sheeted granites form buckles in some New England quarries; Nichols, 1980), these are more widely spaced and not as well developed as sedimentary layering. Thirdly, pop-ups, should they occur, are less likely to be recognized in shield rocks than in flat-bedded sedimentary rocks. Hence although the recent stress history of the Paleozoic cover and the shield rocks has been similar, pop-ups have so far been found only in the cover rocks.

Of particular interest in connection with the pop-ups was the historic occurrence of a similar feature near Westover (discussed above), and the anomalous occurrence of frequent (about three per year), shallow ($<$ 2 km), and small (magnitude 0.3 to 3) earthquakes in Burlington, Ontario, near known pop-ups (Table 2D) and young thrust faults (Table 2E) (Wetmiller, 1980), which suggest that the pop-ups may be related to low-level seismicity in the area.

<u>Bedrock folds and thrust faults of uncertain age</u>

The Paleozoic sediments that cover the shield rocks of southern Ontario and the St. Lawrence lowlands are generally nearly flat-lying and undisturbed. It is therefore remarkable that in some places there are thrust faults of small displacement and small, sharp folds with dips of 20° or more that cannot be attributed to an inital, depositional dip (Table 2E). In some places the folds are probably glacial or pre-glacial in age, but as all the folds and faults in Table 2E appear to have formed near the surface, they are all probably young (?<3 m.y. based on an estimate of continental erosion) relative to the age of the sediments.

Where the folds can be traced to depth, they appear to die out, suggesting to some observers that the origin of the disturbance came from above. A mechanism of glacial ice-thrusting, whereby bedrock frozen to the base of an ice sheet can be thrust and folded by the forward movement of the ice (Karrow, 1963; Durand and Ballivy, 1974) might explain some of the folds. Alternatively the features may be caused by the high horizontal stresses released at the surface, as in many places they resemble pop-ups but lack topographic expression.

If the features represent ice-thrusting, north-south compression (in Ontario) might be expected; if high horizontal stresses, east-west compression. The scatter of results (Fig. 10E) suggests that features of both origins are included, but until the morphology and age of the features are studied in more detail, it is not possible to determine the significance of the slight east-west tendency in the compression directions.

Low-angle slickensides representing strike-slip faulting occur on reactivated normal faults in the St. Lawrence lowlands (Saull and Williams, 1974). New observations by Adams in 1980 indicate the slickensides at the Ottawa River Parkway site lie on the calcite-coated plane of a normal fault that strikes 152° and dips 75°W. The individual striae are 50 to 120 mm long and are sub-horizontal, dipping within $\pm$ 10° of the horizontal with perhaps a slight northward plunge. They therefore appear to represent compression in the quadrant containing the 150° direction, but the age of the movement is not known.

Joint Orientation

Joints in rocks at the earth's surface belong commonly to one of two steeply dipping joint sets (or to a third, subhorizontal set). If the steeply-dipping joints formed as Mohr-type fractures in the two dimensional plane parallel to the earth's surface, then the compression is in the direction of the bisector of the smaller angle between the sets (Scheidegger, 1979). However on the surface of the earth the two sets of steeply dipping joints are more nearly orthogonal than the Mohr fracture theory predicts. There is thus an ambiguity in determining the smaller angle, and so the deduced compression direction may be incorrect by 90°. Despite this, where joint orientations in active tectonic regions (Barbados, European Alps) have been analysed, the derived compression directions are similar to those shown by other indicators (Scheidegger, 1980a).

Scheidegger (1977, 1980b) has analysed the orientation of "fresh" joints from nine sites in southern Ontario (Fig. 8). The joints are fresh in that they are "planar and smooth as if cut by a knife in cheese. They have no fillings, no slickensides, no evidence of any motion at all" (Scheidegger, 1979). The joint orientations are similar in both the Paleozoic and shield rocks and, because of their "freshness", Scheidegger considered the joints to represent contemporary stresses. The southern Ontario results (Scheidegger, 1980b) give the azimuth of each joint set (the mean azimuth of the two joint sets is given in Table 2F in the form xxx ; yyy) and their 90% confidence interval, from which the smaller angle was determined by subtraction and northwest-southeast compression deduced. However when the 90% confidence intervals are considered, only one of the angles is significantly smaller than 90° and so there is an uncertainty as to which direction - NW or NE - is compressional and which tensional. The consistency rather than the accuracy of the results favours northwest-directed compression, although it should be noted that the dominant structural trends in the region probably result from northwest-directed compression during the Precambrian.

Patterns of river drainage are probably controlled in part by joints and other deep structures in the shield, and Scheidegger (1980b) has shown that the orientation of valleys provides substantially the same information as the orientation of joints measured at the surface, though unfortunately with the same 90° ambiguity in the deduced direction of compression.

The value of the compression directions derived from joint analysis has not yet been established for the shield environment, and so Scheidegger's interpretation of joint orientations and indeed the applicability of the method, is open to question. The key problem is whether the joints are indeed forming today as the result of contemporary compression and are being exposed by erosion as they are formed, or whether the joints represent relict stresses imprinted on the rocks in the distant past (Engelder and Geiser, 1980), or both. Until the age of the joints is established the value of any stress orientations they may record is uncertain.

Summary of stress directions from surficial features

The orientation data from Tables 2A to F is presented as summary orientation diagrams in Figure 10. Table 3 gives the mean compression directions and their standard deviations. As can be seen from the diagrams, the inferred directions of maximum compressive stress from stress measurements and quarry-floor buckles suggest a NE-SW orientation on average, while postglacial faults suggest north-south compression, as do pop-ups, although they show a considerable scatter. The orientation of bedrock faults and folds also show considerable scatter, but are slightly biassed towards east-west compression, and the joints ambiguously indicate either northeast or southeast compression. All the mean orientations are subject to large errors (standard deviations of 15 to 30°; Table 3), but nevertheless there is a strong indication that the postglacial features record a compressive stress field (~000°) different from the contemporary field (~045°).

The anomalous orientation of the postglacial field might be explained if those features formed soon after deglaciation and at this time the transient stress field due to crustal flexure (see later in this paper) dominated the "permanent" northeast field. Work on the identification of the stress fields and further analysis of surface stresses following deglaciation in eastern Canada is continuing at the Earth Physics Branch.

CONTRIBUTORS TO INTRAPLATE STRESSES

Plate Tectonics

In regions where locally-induced stresses are not appreciable, intraplate stress calculations based on finite element techniques (with applied stresses along plate boundaries) can generate a regional stress pattern that is comparable to geologically inferred patterns. Boundary stress patterns for the North America plate and the associated orientation of the maximum and minimum principal stress components are shown in Fig. 11. This particular model (portion of Model E 31 of Richardson et al., 1979) has boundary stresses of 10 MPa, with viscous drag force along the base of the lithosphere opposing plate motion, as shown schematically in Fig. 12.

There is general agreement between the stress patterns shown in Fig. 11 and actual stress patterns for much of the conterminous United States (Zoback and Zoback, 1980). The uniform ENE-WSW stress field shown by Sbar and Sykes (1973, 1977) for northeastern United States earthquakes appears to be due to two stress systems, one associated with spreading at the mid-Atlantic ridge and the other, to a viscous drag force along the base of the continent (e.g. see Zoback and Zoback, 1980; Wesnousky and Scholtz, 1979, 1980). The stress pattern predicted by this model for eastern Canada varies gradually from an ENE direction in Quebec to a NE direction in Manitoba.

The lack of a more-or-less uniform orientation for the maximum horizontal stress component in much of eastern Canada may be due to local or regional stresses in certain regions predominating over plate tectonic stresses. More fault-plane solutions of eastern Canadian earthquakes are required for a detailed regional coverage of the deviatoric stress components at mid-crustal depth to see if mid-crustal stresses are dominated by deglacial, plate tectonic or other stresses. For example the stresses associated with deglaciation such as that due to crustal flexure are likely to be much more pronounced and significant in eastern Canada than in the contiguous United States.

Erosion, cooling, incomplete isostatic compensation and postglacial heating

In order to derive general changes or tends in the stress field due to erosion and associated phenomena, consider the idealized profile shown in Fig. 13. For tractability of calculations, the free surface is assumed to be spherical and the lateral boundaries are radial so that the solid angle subtended by the erosional surface remains unchanged. (For the more complicated case of subsidence or uplift with a fixed peripheral boundary, the reader is referred to Price, 1974). During the erosional process, an element at depth of ΔR_E undergoes a change in deviatoric stress. The newly exposed surface experiences thermoelastic extensional stresses due to cooling. In Canada any subsequent erosional isostatic uplift has also been perturbed by episodes of glaciation and deglaciation. For this reason and also because of the lateral gradient in postglacial uplift, stress changes aassociated with isostatic uplift are difficult to treat in a quantitative manner. Subsequent postglacial heating generate thermoelastic compressional stresses.

Erosion

Owing to removal or erosion of a layer of thickness, ΔR_E, an element in the newly exposed surface undergoes (i) a decrease in the vertical component of stress, $\Delta\sigma_V$ by an amount $\bar{\rho} g \Delta R_E$ where $\bar{\rho}$ is the average overburden density and g, the acceleration due to gravity and (ii) a decrease in the horizontal component of stress, $\Delta\sigma_H$ of magnitude $[\nu/(1-\nu)]\rho g \Delta R_E$, where ν is Poisson's ratio. Thus the deviatoric or nonhydrostatic change in stress $\Delta\sigma_E^D$ due to removal of overburden is (Haxby and Turcotte, 1976).

$$\begin{aligned}\Delta\sigma_E^D &= \Delta\sigma_H - \Delta\sigma_V \\ &= [-\nu/(1-\nu)]\cdot[\bar{\rho} g \Delta R_E] - [-\bar{\rho} g \Delta R_E] \\ &= [(1-2\nu)/(1-\nu)]\cdot\bar{\rho} g \Delta R_E \qquad \text{. . .(4)}\end{aligned}$$

Since Eq. (4) is positive, the newly exposed element has undergone a deviatoric compression due to erosion. A physical interpretation of Eq. (4) is as follows. The removal of overburden results in a vertical strain, which in turn would induce a horizontal strain if the lateral boundaries were not constrained laterally. But because of the boundary conditions, there is a deviatoric stress change of an amount represented by Eq. (4). The Earth is considered capable of storing such remanent stresses over geologic time periods of 10^6 - 10^9 yrs (e.g. see Turcotte and Oxburgh, 1976; Minster and Anderson, 1980; McNutt, 1980; Lambeck, 1980).

Cooling

The exposed surface undergoes a thermoelastic stress, $\Delta\sigma_{Th}$, due to a change in temperature, ΔT (Haxby and Turcotte, 1976).

$$\Delta\sigma_{Th} = \frac{\alpha_L E \Delta T}{(1-\nu)} \qquad \text{. . .(5)}$$

where α_L is the linear coefficient of thermal expansion and E, Young's modulus. An alternative but equivalent form of Eq. (5) for the case of thermoelastic cooling is (Haxby and Turcotte, 1976).

$$\Delta \sigma_c = - \frac{\alpha_L E}{(1-\nu)} \left\{ \frac{Q_M \Delta R_E}{k} + \frac{b Q_C}{k} \left[1 - \exp\left(\frac{-\Delta R_E}{b} \right) \right] \right\} \quad \ldots (6)$$

where Q_M and Q_c are the mantle and crustal contributions to heat flow, k is the thermal conductivity, b is the scale depth (of the order of 10 km), and the rest of the parameters are as defined previously.

Isostatic rebound

Isostatic compensation associated with erosion effects a change in the horizontal component of the stress field by an amount

$$\Delta \sigma_{IC} = -f \frac{E}{(1-\nu)} \frac{\bar{\rho}}{\rho_M} \frac{\Delta R_E}{R_E} \quad \ldots (7)$$

where the subscript IC stands for isostatic compensation, f the fraction of isostatic compensation achieved, ρ_m the density of the upper mantle, R_E the radius of the earth and the other symbols are as defined previously. In the absence of any external (perturbing) stresses such as ice loads, isostatic compensation associated with erosion should be complete, i.e. f=1, because of the lengthy time span involved. Isostatic uplift associated with an eroded layer of thickness ΔR_E is $(\bar{\rho}/\rho_m) \Delta R_E$.

A smoothed free-air gravity map of eastern Canada shows that the central part of the region once covered by the Laurentide ice sheet has anomalies of up to -50 milligals. These negative anomalies suggest overcompensation and that a substantial amount of uplift has yet to occur (Walcott, 1970). A hypothetical uplift curve by Walcott shows that 200 m of uplift has occurred in the central region and that 350 m more of uplift remains. Although Walcott (1977) still claims that the very close coincidence of the gravity anomaly in both shape and position with the region of uplift suggests a close relationship and supports a large amount of remaining uplift, others (e.g. Cathles, 1975) have considered the association coincidental and have considered that a maximum of only 35 m of uplift will occur. An intermediate estimate of 160 m, which was made by Andrews (1970a) from the extrapolation of uplift history curves, is independent of the interpretation of the gravity anomaly field. However Cathles' (1975, Appendix VII) recalculation from Andrew's data suggests a maximum of only 23 m.

Although the amount of uplift remaining is not established, we adopt Walcott's maximum value of 350 m as the largest possible amount remaining. We can then place (maximum) constraints on f and ΔR_E in Eq. (7) for the case where the resultant stress, $\Delta \sigma_R$ in Eq. (9), is positive, which is the case of interest in this study.

Postglacial heating

Thermoelastic stress associated with postglacial heating, $\Delta \sigma_P$, is

$$\Delta \sigma_P = \frac{\alpha_L E \Delta T}{(1-\nu)} \quad \ldots (8)$$

where the symbols are as described previously.

Resultant stress

Since each of the three processes is considered to be linear, the individual contributions can be summed so that the resultant stress field, $\Delta\sigma_R$, is

$$\Delta\sigma_R = \frac{1-2\nu}{1-\nu}\bar{\rho} g \Delta R_E - \frac{\alpha_L E}{(1-\nu)}\left\{\frac{Q_M \Delta R_E}{k} + \frac{bQ_C}{k}\left[1 - \exp\left(\frac{-\Delta R_E}{b}\right)\right]\right\} - f\frac{E}{(1-\nu)} \cdot \frac{\bar{\rho}}{\rho_M} \cdot \frac{\Delta R_E}{R_E} + \frac{\alpha_L E \Delta T}{(1-\nu)} \quad \ldots (9)$$

Fig. 14(a) illustrates how $\Delta\sigma_R$ [Eq. (9)] varies with thickness of eroded layer, ΔR_E, for the limiting case where f=0, and Fig. 14(b) for the case where f varies from 0 to 1. In Fig. 14(a) the individual contributions from erosion $\Delta\sigma_E^R$ [Eq. (4)], cooling $\Delta\sigma_C$ [Eq. (6)], and postglacial heating $\Delta\sigma_P$ [Eq. (8)] are shown for representative values for parameters of the Canadian Shield that are listed in Table 4. Here, for f=0, the large component of deviatoric compression from erosion is largely (75%) offset by the concomitant extensional stress component due to cooling, with the relatively smaller contribution from postglacial heating making the resultant slightly more compressive. Fig. 14(b) shows the effect upon $\Delta\sigma_R$ of varying proportions of isostatic compensation (f=0 to 1). Based on Fig. 14(b) and the remaining uplift associated with the Wisconsin Glaciation as estimated by Walcott (1970) and discussed above, we can place upper limits on f and ΔR_E for the case where $\Delta\sigma_R > 0$. From Fig. 14(b), f must be less than 1/3 for $\Delta\sigma_R$ to be greater than zero. For the extreme case where the residual uplift is 350 m (over Hudson Bay), ΔR_E must be less than about 600 m for f = 1/3 and $\Delta\sigma_R > 0$. That is on the Canadian Shield $\Delta\sigma_R$ associated with the erosion process and perturbed by glacial ice loading and unloading attains its maximum positive value in the Hudson Bay area for the case where the thickness of the eroded layer is less than about 600 m, and $\Delta\sigma_R$ should decrease towards the periphery of the area formerly occupied by the Laurentide ice load. Consequently phenomena other than that of erosion are required to explain the presence of a high horizontal stress field that exists throughout the Canadian Shield.

Stresses related to glaciation and associated phenomena

(i) Postglacial heating

Fig. 14(a) indicates that the contribution to the horizontaL stress field from postglacial heating is of the order of a few MPa and is compressive. This amount is insignificant when compared to the individual contributions from erosion and the associated cooling, assuming these stresses have been "frozen-in" and not released during uplift and erosion, but may become significant when compared to the sum of the latter two components. In connection with postglacial heating effects, it is worth noting that Gilbert (1886) originally attributed postglacial anticlines (pop-ups) in New York State to "expansion as the surface rocks recovered from the cold of the glacial period", although this explanation is not now generally accepted.

(ii) Repeated glaciation and de-glaciation

It has been hypothesized by Lee (1978) that, under the assumption of rigid confinement, repeated glacial loading-unloading cycles can generate a residual horizontal compressive stress field, $\Delta\sigma_G$, in much of eastern Canada. Subject to the boundary condition stated above, the residual stress field after the retreat of the ice load is (Lee, 1978).

$$\Delta\sigma_G = F\left[\frac{E}{(1-\nu)}\cdot\Delta\epsilon_v\right]$$

where F stands for a (undetermined) fraction of the vertical component stress field (in brackets) resulting from the ice load that causes a vertical strain, $\Delta\epsilon_v$. It has been suggested that due to visoelastic after-effects, a residual horizontal stress field remains after the ice load has retreated and that repeated load-unload cycles result in a cumulation of the individual contributions. Furthermore, it has been suggested (by Lee and Asmis, 1979) that the manner in which the Laurentide ice sheet appears to have retreated could generate a horizontally anisotropic stress distribution, that is one for which there is a greater horizontal stress component in an EW direction than in a NS direction.

(iii) Shear strain due to differential postglacial uplift

Consider, for example, the Canadian Shield lying between Lake Ontario and Hudson Bay. Based on Fig. 2 of Andrews (1970b), during the past 12,000 years a shear strain, φ, of the order of 3 x 10^{-4} should accumulate in this region. For shield rocks the modulus of rigidity, G, is of the order of 2-4 x 10^{-6} MPa (see Birch, 1966). The average shear stress, τ, where τ=Gφ, is of the order of 10 MPa. However, localized stress or strain concentrations due to a non-uniform ice load (e.g. see Peltier et al., 1978; Clark, 1980) or a moving ice sheet or weak rocks could result in regions of higher stress concentration (N.H. Sleep, personal communication, 1981).

(iv) Lithospheric flexure due to deglaciation

Stein et al. (1979) have proposed that lithospheric flexure due to the removal of an ice load generates stresses able to account for the deviatoric stress patterns (see Fig. 7) of northeastern Canada earthquakes, that is deviatoric extension (in the northeast-southwest quadrants) for earthquakes occurring under Baffin Bay and deviatoric compression (in the same quadrants) for events on Baffin Island. Consider a semi-infinite ice load, with a boundary along the western edge of Baffin Bay and extending westwards, resting on an elastic lithosphere that is underlain by a fluid asthenosphere. Fig. 15 shows the expected (steady-state) quadrantal stress pattern when the ice load is removed. This simplified model predicts thrust faulting under Baffin Bay and normal faulting under Baffin Island at shallow depths, in general agreement with Fig. 7 and deviatoric horizontal stresses of the order of 10 MPa at mid-crustal (~20 km) depth and 15 MPa at the surface.

It would appear that the stress environment in the Baffin Island-Baffin Bay area is the superposition of contributions from several phenomena. In additional to flexural stresses due to removal of an ice load, there are gravitationally-induced stresses due to lateral variations in topography and crustal thickness, and shear stresses due to continuing differential uplift. There is a steep gradient in the free-air gravity anomaly field in this region that correlates with seismicity (Basham et al., 1977; Forsyth, 1981), as shown in Fig. 16 and with differential postglacial uplift (Andrews, 1970b). Further measurements such as in situ stress determinations and more earthquake fault-plane solutions are required for a better understanding of the role played by each of the above phenomena in the seismotectonics of this region.

(v) Stresses near edge of ice sheet

Of primary importance to the safe storage of radioactive waste over a long time span (thousands of years) in any bedrock vault is the largest change in stress level that will affect the vault. In eastern Canada, the largest changes expected would be due to the advance or retreat of an ice sheet and would occur near the edge of the moving sheet. However, only the static case can be treated simply.

Fig. 17 shows a schematic profile of an ice front resting on an elastic lithosphere, which in turn is floating on a liquid asthenosphere. The formulation outlined in Walcott (1970) is used to calculate the maximum induced stress at the shallow depth of 1 km. Under an ice load of 2 km in thickness, the maximum change in the horizontal component of stress occurs several hundred kilometres behind the ice front (i.e. under the ice) and is of the order of +20 MPa, i.e., compressive. At this location the ice load is about 15 MPa. Therefore the deviatoric horizontal stress is +5 MPa and is compressive. However, in advance of the ice front, the greatest change in the horizontal stress component occurs 50 km from the ice front and is about -25 MPa, i.e., extensional. Thus, for an ice load of 2 km in thickness, the induced stress field at shallow depths favours a thrust faulting regime under the ice load and a normal, or even tensional, fault regime in advance of the ice sheet. South of Hudson Bay, these faults would tend to strike east-west (assuming main loading mass over Hudson Bay). Thus a vault overrun by a 2 km thick ice load and then reexposed would experience a change in the deviatoric stress field of about 30 MPa at shallow ($\sim$1 km) depths.

There is evidence of rock failure due to stress changes associated with deglaciation. Morner (1978) presents for Fennoscandia evidence that indicates the maximum rate of glacio-isostatic uplift occurring at about the time of deglaciation, is related to intense faulting and fracturing of bedrock.

Gravitationally induced stresses

Lateral variations in crustal or lithospheric thickness are considered by some to be the main source of the crustal stress field (e.g. Dewey and Bird, 1970,; Artyushkov, 1973). Theoretical calculations (Simmons et al., 1978) of shear stress at mid-crustal depth due to pronounced topography indicate a strong correlation between the steep gradient in the free-air gravity anomaly field, stress concentration of the order 10 MPa and seismicity in the Puget Sound region of northwestern United States. A similar situation could be present along Baffin Island; Fig. 16 shows that earthquakes in northeastern Canada occur where there are steep gradients in the free-air gravity contours (e.g. see Wetmiller and Forsyth, 1981). However the converse does not always hold; there are regions of steep gradients where earthquakes have so far not been detected. At continental-oceanic margins, shear stress concentrations at mid-crustal depths of several tens of MPa are indicated by finite element techniques (e.g. see Bott and Dean, 1972; Kusnir and Bott, 1977). Uncompensated sedimentary loading along the continental margin bordering the Beaufort Sea can generate horizontal deviatoric extensional stresses of several tens of MPa at a depth of $\sim$40 km (Hasegawa et al., 1979). Gravitationally-induced stresses of several MPa at structural boundaries between geologic provinces within the Canadian Shield are indicated by the finite element calculations of Goodacre and Hasegawa (1980). These induced stresses are associated with a gravity anomaly of up to 100 mgal (1 mgal = 10^{-5} m s^{-2}) across the structural boundary and may contribute to the seismicity in the Charlevoix and Lower St. Lawrence seismic zones.

Vertical intrusions

Stress anomalies near intrusions can occur in several different ways: vertical intrusions in a homogeneous plate subjected to a uniform horizontal applied stress field, intrusions with marked density contrast with the surrounding medium, and inclusions for which stresses generated at each major cycle of development are retained, and they can contribute to regional stress anomalies. Theoretical calculations of regional stress in or near intrusions within a continental crust indicate that, for inclusions stiffer than the surrounding crust, stress concentration of only 20 or 30 percent above regional values are likely but for weakened intrusions (e.g. by serpentinization) stress concentrations of more than 200 percent above the regional may occur just outside the periphery of the inclusion (Campbell, 1978). Preliminary finite element calculations of gravitationally induced stresses due to a density contrast between intrusion and surrounding material indicates a weakening of a less dense intrusion and strengthening of a more dense intrusion within the upper part of the intrusion (A.K. Goodacre, written communication, 1980).

Thus, differences in elastic parameters and in density contrast between an intrusion, such as a pluton intrusion, and surrounding medium can generate a stress concentration within or adjacent to the intrusion. The question of whether gravitationally induced stresses or anomalous stress concentrations due to differences in elastic parameters are more pronounced depends on the degree of mismatch between density and elastic parameters. When the complete history of an intrusion is considered, the treatment of Price (1979) indicates appreciable remanent stress concentrations within an intrusion, with the possibility of tensional fractures being developed; the stresses considered are due to thermoelastic processes, erosion, and shearing associated with deglaciation.

From a seismological point of view, caution should be exercised when drawing conclusions about stress concentrations due to intrusions. A superposition of epicenters on gravity anomaly maps indicate that plutonic intrusions in eastern Canada (e.g. see Forsyth, 1981) and in eastern United States (M.F. Kane and R.W. Simpson, personal communication, 1980) tend to be relatively nonseismic when compared to the surrounding crust. An obvious inference is that intrusions tend to be more homogeneous and less fractured than the surrounding host material (if intrusions are late or post orogenic). However, this does not imply that plutonic intrusions are completely free of major or minor faults and fractures (e.g. see Mair and Green, 1981).

POSSIBLE EARTHQUAKE TRIGGER MECHANISMS

Trigger mechanisms of shallow intraplate earthquakes are discussed briefly with reference to the Coulomb-Mohr failure criterion (e.g. see Fig. 3). The region of interest is a weakened region that is on the verge of failure, as illustrated in Fig. 18a. That is, the Mohr circle is close to the Coulomb failure line.

The following cases are discussed very briefly:

(i) stress readjustment due to previous earthquakes
(ii) stress concentration due to faults and cracks
(iii) static fatigue and hydrolytic weakening
(iv) variation in pore pressure
(v) earth tides

(i) Stress adjustment due to previous earthquakes

Large earthquakes tend to modify the stress-strain regime over an extended region and consequently could contribute to the triggering of earthquakes in neighboring regions (e.g. see Mogi, 1969). Aftershock activity tends to modify the stress-strain regime close to or on the main fault. Stress drops during earthquakes in the Canadian Shield are of the order of 5 MPa across the fault plane. The corresponding variation in the stress-strain regime surrounding the fault depends upon a number of factors: fault dimensions, including average dislocation across the fault; fault orientation; nature of crust surrounding the fault; and hypocentral distance.

Only recently have migration rates of crustal deformation due to a large earthquake been determined and these are in interplate tectonic areas. Kasahara (1979) for example, has estimated this velocity of migration of the sudden strain change (maximum shear strain of the order of 10^{-6}) to vary from 10 to 100 km/yr.

(ii) Stress concentrations due to faults and cracks

Stress concentrations due to faults occur on a macroscopic and microscopic scale. Large earthquakes in south central Soviet Union tend to occur at the junction of faults or lineaments (on the $10^4 - 10^5$ m scale). Stress concentrations near faults have been measured in Canada (on the 1-10 m scale) (e.g. see Herget, 1980). On a much smaller scale ($\ll$1 m) considerable stress concentration can occur at the tip of cracks (e.g. see Jaeger and Cook, 1971). The relation between the stress field induced by cracks and the occurrence of earthquakes has been discussed by Niewiadomski and Ritsema (1980). Thus cracks and faults not only modify the ambient stress field but also are regions where initial failure generally occurs.

(iii) Static fatigue and hydrolytic weakening

The chemical effects of water at crack tips, where there is a high stress concentration, can weaken the rocks and thus trigger an earthquake (e.g. see Kisslinger, 1976; Kirby, 1980). The effect of this process is either to lower the frictional characteristics of the rock, as illustrated in Fig. 18c, or to lower the effective cohesive strength of the rock, as shown in Fig. 18d. Water reacting with quartz can produce a chemical weakening of the silicates (hydraulic weakening) resulting in intracrystalline slip (e.g. see Kirby, 1980). The formation of a fault gouge results in a decrease in the coefficient of friction as shown in Fig. 18c (e.g. see Logan, 1975; Kirby, 1980; Hanks and Raleigh, 1980).

(iv) Variation in pore pressure

Fluid injection, reservoir impounding and fluctuation in hydrostatic head (ground water level change) can, under certain circumstances, trigger earthquakes. Fluid injection has triggered earthquake activity in Denver and Rangely, Colorado (Healey *et al.*, 1968; Raleigh *et al.*, 1972). Water percolating through joint systems after start of filling of the Manic 3 reservoir and the LG2 reservoir in Quebec triggered a long sequence of induced earthquakes (Leblanc and Anglin, 1978; Anglin and Buchbinder, 1980). A small long-term fluctuation in water table elevation triggered two (Richter magnitudes 5.9 and 6.9) shallow-focus earthquakes in western Australia (Denham *et al.*, 1980). A 1 m head change could cause pore pressure changes of 0.01 MPa. Theory indicates that a weakened zone or fault on the verge of failure must be present nearby if seismicity is to result. With respect to the Coulomb-Mohr diagram shown in Fig. 18b, the increase in pore pressure, ΔP, decreases the effective normal stress so that the Mohr circle shifts to the left and contacts the failure line. The complicated role of pore pressure concerning the mechanics of earthquake triggering is discussed by Lachenbruch (1980).

(v) Earth tides

There is still no concensus as to the degree of correlation between earth tides and the occurrence of earthquakes. A cross-correlation of the occurrence of 9000 California earthquakes with earth tides indicated a random association (Knopoff, 1964). The reasons given for this lack of correlation can be explained with reference to Fig. 19. The small 0.001 - 0.005 MPa stress induced by earth tides (M_2), with a periodicity of 12 hours does not, in general, have a long enough duration to act as an efficient trigger mechanism. Consequently, earth tides would have to act over days and possibly weeks before triggering earthquakes and hence, no synchronization with tidal periods is to be expected. However, it appears that under favorable circumstances, earth tides can trigger earthquakes. Theoretical calculations by Heaton (1975) indicate that shallow (less than 30 km) focus, larger-magnitude earthquakes with oblique-slip or dip-slip focal mechanisms are favorable for triggering by earthtides. A strong correlation was found between earth tides and the occurrence of earthquakes in an area of complex faulting in northeastern California (Mohler, 1980). The favorable conditions under which this occurred were that the region has weakened zones on the verge of failure, the medium was relatively homogeneous with parallel faults and the stresses induced by earth tides tended to decrease the normal stress and increase the shear stress acting along the faults, thereby triggering earthquakes.

In eastern Canada, the role of earth tides in triggering earthquakes is unknown. An indirect test between earth tides and changes in seismic velocities in the Charlevoix seismic zone was made by Buchbinder (1981); the hypothesis that the vertical component of the earth tide produces changes in travel-time was tested experimentally and rejected. An approximate calculation indicates that the maximum induced stress, which is due to the semi-diurnal lunar (M_2) tide, is of the order of 0.001 MPa in the Charlevoix Zone (D.R. Bower, personal communication, 1980).

SUMMARY AND DISCUSSION

General properties of the stress field in eastern Canada are as follows:

(i) from the surface down to mid-crustal depths, available data indicate the maximum horizontal stress component is greater than the vertical. This implies a thrust-fault or strike-slip fault seismotectonic environment, which is similar to that in the contiguous northeastern United States (c.f. Herrmann, 1979).

(ii) in situ stress measurements and inferences from surficial features indicate a bimodal distribution in the direction of maximum principal stress; contemporary geologic features and some localized in situ stress measurements indicate compression about an east-west direction with a scatter of $\pm 45°$ whereas postglacial features indicate north-south compression.

(iii) there is an appreciable scatter in the direction of the deviatoric compression vector of eastern Canada earthquakes because of the inherent (possibly large) uncertainty in inferring principal stress directions from fault-plane solutions, and consequently more fault-plane solutions of eastern Canada earthquakes are required to determine (on a statistical basis) whether or not there is a uniform stress field at mid-crustal depths. The present data cannot rule out the possibility of a uniform stress field at this depth.

(iv) plausible phenomena or mechanisms for the high horizontal stress component in eastern Canada are as follows: plate tectonics, postglacial heating, successive glaciation-deglaciation, and possibly the erosional process in certain regions (e.g. near Hudson Bay).

(v) stress concentrations can result from (a) contrast of density and elastic parameters between intrusion and host rock (b) lateral variations in crustal density (c) pronounced topography (d) presence of faults and cracks (e) flow of groundwater (f) crustal flexure due to glaciation and deglaciation (g) differential postglacial uplift.

As a step towards understanding earthquake phenomena in eastern Canada, in particular to earthquake prediction possibilities in an intraplate environment, the Charlevoix seismic region has been selected for continuing experiments on physical processes related to earthquakes (see Whitham, 1979). To date the following experiments have been performed: explosion studies to detect significant changes in P-wave velocity (Buchbinder and Keith, 1977); measurement of magnetotelluric fields for a three year period (Kurtz and Niblett, 1980); continuous tilt and strain observations at a crustal deformation observatory (Labrecque et al., 1979); and large-scale slow deformation monitored by a network of nano-gravity meter stations (Lambert et al., 1979). First order relevelling along the north shore of the St. Lawrence

River is also planned on a semi-annual basis, and a geodetic network has been established to measure lateral earth movements (Jones, 1970).

The integration of data from various disciplines is improving our knowledge of the stress field. This information, in turn, is enhancing our understanding of the seismotectonics and glacial-deglacial phenomena in eastern Canada.

ACKNOWLEDGEMENTS

The authors are grateful to J.L. Wallach of A.E.C.B. for encouraging them to write a report on the talks (on the fundamental causes of the neotectonic conditions in eastern Canada) they presented at A.E.C.B. in Ottawa on November 17 and 18, 1980. The authors thank the following for sending requested information: I. Ermanovics of G.S.C. for a write-up of the talk he presented at this meeting; P. Lecomte of Quebec Hydro for a report on stress measurements in the Lac Beauchêne, Témiscamingue region of Quebec; J. Bowlby of Ontario Hydro for providing information on folds in Southern Ontario; J. Levay of SEBJ for stress measurements at LG-2 (north-western Quebec); E.M. Taylor of Ontario Hydro for a reference list of papers on stress measurements in southern Ontario; and J.A. Franklin of Morton & Partners for reports on stress measurements. A discussion with W.F. Brace of M.I.T. has given the authors insight into lower and upper bounds on in-situ stress measurements and a discussion with G. Herget of CANMET on the variability in azimuth of the maximum principal stress as determined from in-situ stress measurements has been helpful.

The authors appreciate the many helpful comments on both the scientific contents and the grammatical structure of this manuscript from their colleagues at EPB, namely to M.J. Berry, P.W. Basham, M.R. Dence, D.A. Forsyth, A.K. Goodacre, A.G. Green, A.M. Jessop, A. Judge, A. Lambert and A. Taylor.

REFERENCES

Adams, J. 1981. Postglacial faulting: a literature survey of occurrences in eastern Canada and comparable glaciated areas. Atomic Energy of Canada Technical Record 142, 63 pp.

Aki, K. and Richards, P.G. 1980. Quantitative seismology - Theory and Methods, Vol. 1., 38-60, W.H. Freeman and Company, San Francisco.

Andrews, J.T. 1970a. Residual uplift. In A geomorphological study of post-glacial uplift with particular reference to Arctic Canada. Institute of British Geographers, London, Chapter 9, 125-132.

Andrews, J.T. 1970b. Present and postglacial rates of uplift for glaciated northern and eastern North America derived from postglacial uplift curves. Can. J. Earth Sci., 7, 703-715.

Anglin, F. and Buchbinder, G. 1980. Microseismicity in the mid St. Lawrence Valley Charlevoix Zone, Quebec. (Submitted for publication).

Artyushkov, E.V. 1973. Stresses in the lithosphere caused by crustal thickness inhomogeneities. J. Geophys. Res., 78, 7675-7708.

Basham, P.W., Forsyth, D.A. and Wetmiller, R.J. 1977. The seismicity of northern Canada. Can. J. Earth Sci., 14, 1646-1667.

Basham, P.W., Weichert, D.H., and Berry, M.J. 1979. Regional assessment of seismic risk in eastern Canada. Bull. Seism. Soc. Am., 69, 1567-1602.

Benson, R.P., Kierans, T.W., and Sigvaldson, O.T. 1970. In situ and induced stresses at the Churchill Falls underground power house, Labrador - Proc. 2nd Congress Int. Soc. Rock Mech., 2, 821-832.

Berry, M.J. and Hasegawa, H.S. 1979. Seismic risk and toxic waste disposal: a discussion. Geoscience Canada, 6, 195-198.

Birch, F. 1966. Compressibility; Elastic Constants. In Handbook of Physical Constants, edited by S.P. Clark. Geological Soc. of Am., Memoir 97, 97-173.

Bird, G.W. 1979. Geochemistry of radioactive waste disposal. Geoscience Canada, 6, 199-204.

Bott, M.H.P. and Dean, D.S. 1972. Stress systems at young continental margins. Nature Physical Science, 235, 23-25.

Bott, M.H.P. and Kusznir, N.J. 1979. Stress distributions associated with compensated plateau uplift structures with application to the continental splitting mechanism. Geophys. J.R. astr. Soc., 56, 451-459.

Brace, W.F. and Kohlstedt, D.L. 1980. Limits on lithospheric stress imposed by laboratory experiments. J. Geophys. Res., 85, 6248-6252.

Buchbinder, G.G.R. and Keith, C. 1977. Search for changes in velocity in the La Malbaie region of Quebec. Trans. Am. Geophys. Union, 58, 432 (abstract).

Buchbinder, G.G.R. 1981. Velocity changes in the Charlevoix region, Quebec. (Accepted for publication in Maurice Ewing Prediction Symposium A.G.U. 1981).

Burridge, R. and Knopoff, L. 1964. Body force equivalents for seismic dislocations. Bull. Seism. Soc. Am., 54, 1875-1888.

Caley, J.F., 1941. Paleozoic geology of the Brantfield area, Ontario. Geological Survey of Canada, Memoir 226, 176 pp.

Campbell, D.L. 1978. Investigation of the stress-concentration mechanism for intraplate earthquakes. Geophys. Res. Letters, 5, 477-479.

Carson, D.M., 1981. Preliminary report on the Paleozoic geology of the Peterborough-Campbellford area, Southern Ontario. Ontario Geological Survey Open File Report 5331.

Cathles, L.M. 1975. The viscosity of the Earth's mantle. Princeton University Press, Princeton, 386.

Clark, J.A. 1980. The reconstruction of the Laurentide ice sheet of North America from sea level data: method and preliminary results. J. Geophys. Res., 85, 4307-4323.

Coates, D.F., 1964. Some cases of residual stress effects in engineering work. in Judd, W.R. (ed) State of stress in the earth's crust. Elsevier, New York, p. 679-688.

Commission Hydro-Electrique du Québec. 1967. Mesure des contraintes en place. Centrale Hydro-Electrique du Lac Beauchêne, Témiscamingue. Contrat No. 1009-61.

Dence, M.R. and Scott, W.J. 1979. The use of geophysics in the Canadian radioactive waste programme. Geoscience Canada, 6, 190-194.

Denham, D., Alexander, L.G. and Worotnicki, G. 1980. The stress field near the sites of the Meckering (1968) and Calingiri (1970) earthquakes, Western Australia. Tectonophysics, 67, 283-317.

Dewey, J.F. and Bird, J.M. 1970. Mountain belts and the new global tectonics. J. Geophys. Res., 75, 2625-2647.

Dunbar, W.S. and Garland, G.D. 1975. Crustal loads and vertical movements near Lake St. John, Quebec. Can. J. Earth Sci., 12, 711-720.

Durand, M. and Ballivy, G., 1974. Particularités rencontrées dans la région de Montréal resultant de l'arrachement d'écailles de roc par la glaciation. Canadian Geotechnical Journal 11, 302-306.

Engelder, T., and Geiser, P., 1980. On the use of regional joint sets as trajectories of paleostress fields during the development of the Appalachian Plateau, New York. J. Geophys. Res., 85, 6319-6341.

Ermanovics, I. and Card, K. 1980. Remarks on the tectonics of Precambrian rocks, specifically Superior-Grenville Province a propos SORAM. Presented at A.E.C.B. meeting in Ottawa on Nov. 17, 1980, on "Response of underground mine/repository to seismic activity".

Forsyth, D.A. 1981. Characteristics of the western Quebec seismic zone. Can. J. Earth Sci., 18, 103-119.

Franklin, J.A. and Hungr, O. 1978. Rock stresses in Canada - their relevance to engineering projects. Rock Mechanics, Suppl, 6, 25-46.

Frost, N.H. and Lilly, J.E. 1966. Crustal movement in the Lake St. John area, Quebec. Can. Surveyor, 20, 292-299.

Gilbert, G.K. 1886. Some new geologic wrinkles. Amer. J. Sci., 3rd series, 32, 324.

Goodacre, A.K. and Hasegawa, H.S. 1980. Gravitationally induced stresses at structural boundaries. Can. J. Earth Sci., 17, 1286-1291.

Haimson, B.C. 1978. Hydrofracturing stress measurements, Hole UN-1, Darlington Generating Station, Report No. 78250. Prepared for Geotechnical Engineering Department, Ontario Hydro, pp. 30.

Handin, J. 1966. Strength and ductility. In Handbook of Physical Constants, edited by S.P. Clark. Geological Soc. of Am., Memoir 97, 223-289.

Hanks, T.C. and Raleigh, C.B. 1980. The conference on magnitude of deviatoric stresses in the Earth's crust and uppermost mantle. J. Geophys. Res., 85, 6083-6085.

Hasegawa, H.S., Chou, C.W. and Basham, P.W. 1979. Seismotectonics of the Beaufort Sea. Can. J. Earth Sci., 16, 816-830.

Hasegawa, H.S. and Wetmiller, R.J. 1980. The Charlevoix earthquake of 19 August 1979 and its seismo-tectonic environment. (Accepted for publication in Earthquake Notes).

Hashizume, M. 1973. Two earthquakes on Baffin Island and their tectonic implications. J. Geophys. Res., 78, 6060-6081.

Hashizume, M. 1974. Surface wave study of earthquakes near northwestern Hudson Bay, Canada. J. Geophys. Res. 79, 5458-5468.

Hashizume, M. 1977. Surface-wave study of the Labrador Sea earthquake 1971 December. Geophys. J.R. astr. Soc., 51, 149-168.

Haxby, W.F. and Turcotte, D.L. 1976. Stresses induced by the addition or removal of overburden and associated thermal effects. Geology, 4, 181-184.

Healy, J.H., Rubey, W.W., Griggs, D.T. and Raleigh, C.B. 1968. The Denver earthquakes - Disposal of waste fluids by injection into a deep well has triggered earthquakes near Denver, Colorado. Science, 161, 1301-1310.

Heaton, T.H. 1975. Tidal triggering of earthquakes. Geophys. J.R. astr. Soc., 43, 307-326.

Herget, G. 1980. Regional stresses in the Canadian Shield. In. Proceedings of 13th Canadian Rock Mechanics Symposium, Toronto, May 1980. CANMET, Energy, Mines and Resources, Canada, Division Report MRP/MRL 80-8 (OP), 9-16.

Herrmann, R.B. 1979. Surface wave focal mechanisms for eastern North American earthquakes with tectonic implications. J. Geophys. Res., 84, 3543-3552.

Hodgson, J.H. and Stevens, A.E. 1964. Seismicity and earthquake mechanism. In. Research in Geophysics, edited by H. Odishaw. The M.I.T. Press, Cambridge, Massachusetts, 27-59.

Horner, R.B., Stevens, A.E., Hasegawa, H.S. and Leblanc, G. 1978. Focal parameters of the July 12, 1975, Maniwaki, Quebec, earthquake - an example of intraplate seismicity in eastern Canada. Bull. Seism. Soc. Am., 68, 619-640.

Horner, R.B., Wetmiller, R.J. and Hasegawa, H.S. 1979. The St-Donat, Quebec, earthquake sequence of February 18-23, 1978. Can. J. Earth Sci., 16, 1892-1898.

Jaeger, J.C. and Cook, N.G.W. 1971. Fundamentals of rock mechanics. Chapman and Halls Ltd., pp. 515.

Jamison, D.B. and Cook, N.G.W. 1980. Note on measured values for the state of stress in the Earth's crust. J. Geophys. Res., 85, 1833-1838.

Jessop, A.M. and Lewis, T. 1978. Heat flow and heat generation in the Superior Province of the Canadian Shield. Tectonophysics, 50, 55-77.

Jones, H.E. 1970. Geodetic survey measurements to determine motion in the Earth's crust. In Earthquake displacement fields and the rotation of the Earth, edited by L. Mansinha. Reidel Publishing Company, Dordrecht-Holland, 269-275.

Karrow, P.F., 1963. Pleistocene geology of the Hamilton-Galt area. Ontario Department of Mines, Geological Report 16, 68 pp.

Kasahara, K. 1979. Migration of crustal deformation. Tectonophysics, 52, 329-341.

Kirby, S.H. 1980. Tectonic stresses in the lithosphere: constraints provided by the experimental deformation of rocks. J. Geophys. Res., 85, 6353-6363.

Kisslinger, C. 1976. A review of theories of mechanisms of induced seismicity. Engineering geology, 10, 85-98. Edited by W.G. Milne.

Knopoff, L. 1964. Earth tides as a triggering mechanism for earthquakes. Bull. Seism. Soc. Am., 54, 1865-1870.

Kurtz, R.D. and Niblett, E.R. 1980. Time-dependence of magnetotelluric fields in a tectonically active region in eastern Canada. J. Geomagn. Geoelectr., 30, 561-577.

Kusznir, N.J. and Bott, M.H.P. 1977. Stress concentration in the upper lithosphere caused by underlying visco-elastic creep. Tectonophysics, 43, 247-256.

Labrecque, J.J., Bower, D.R. and Lambert, A. 1979. Mesures de l'inclinaison et de la déformation dans le compté de Charlevoix, P. Québec. (in preparation).

Lachenbruch, A.H. 1980. Frictional heating, fluid pressure, and the resistance to fault motion. J. Geophys. Res., 85, 6097-6112.

Lambeck, K. 1980. Estimates of stress differences in the crust from isostatic considerations. J. Geophys. Res., 85, 6397-6402.

Lambert, A., Liard, J. and Dragert, H. 1979. Canadian precise gravity networks for crustal movement studies: an instrument evaluation. Tectonophysics, 52, 87-96.

Lambert, A. and Vanicek, P. 1979. Contemporary crustal movements in Canada. Can. J. Earth Sci., 16, 647-668.

Lawson, A.C., 1911. On some post-glacial faults near Banning, Ontario. Bull. Seism. Soc. Am., 1, 159-166.

Leblanc, G. and Anglin, F. 1978. Induced seismicity at the Manic 3 reservoir, Quebec. Bull. Seism. Sci. Am., 68, 1469-1485.

Leblanc, G. and Buchbinder, G. 1977. Second microearthquake survey of the St. Lawrence Valley near La Malbaie, Quebec. Can. J. Earth Sci., 14, 2778-2789.

Lee, C.F. 1978. A rock mechanics approach to seismic risk evaluation. In. Proc. 19th U.S. Symp. on Rock Mechanics, 1, 77-88.

Lee, C.F. and Asmis, H.W. 1979. An interpretation of the crustal stress field in northeast North America. Proceedings 20th U.S. Symp. on Rock Mechanics 655-662.

Lindner, E.N. and Halpern, J.A. 1977. In-situ stress: an analysis. In 18th U.S. Symp. on Rock Mechanics, Supplemental volume, held at Keystone, Colorado June 22-24, 1977, 4C1-1 to 4C1-7.

Lo, K.Y., 1978. Regional distribution of in situ horizontal stresses in rocks of southern Ontario. Can. Geotech. J., 15, p. 371-381.

Lo, K.Y., and Morton, J.D. 1976. Tunnels in bedded rocks with high horizontal stresses. Can. Geotech. J., 13, 216-230.

Lo, K.Y. Devata, M., and Yuen, C.M.K. 1979. Performance of a shallow tunnel in a shaly rock with high horizontal stresses. Proceedings, Tunnelling '79, Institute of Mining and Metallurgy, London, England, March 12-16.

Logan, J.M. 1975. Friction in rocks. Reviews of Geophysics and Space Physics, 13, 358-361.

Mair, J.A. and Green, A.G. 1981. Radioactive waste disposal and intra-plate stresses - high resolution seismic reflection profiles across a "homogeneous" granite batholith. (submitted for publication).

Maruyama, T. 1963. On the force equivalents of dynamic elastic dislocations with reference to the earthquake mechanism. Bull. Earthq. Res. Inst., Tokyo Univ., 41, 467-486.

McKenzie, D.P. 1969. The relation between fault plane solutions for earthquakes and the directions of the principal stresses. Bull. Seism. Soc. Am., 59, 591-601.

McGarr, A. and Gay, N.C. 1978. State of stress in the earth's crust. Ann. Rev. Earth Planet. Sci., 6, 405-436.

McNutt, M. 1980. Implications of regional gravity for state of stress in the Earth's crust and upper mantle. J. Geophys. Res., 85, 6377-6396.

Minster, J.B. and Anderson, D.L. 1980. Dislocations and nonelastic processes in the mantle. J. Geophys. Res., 85, 6347-6352.

Mogi, K. 1969. Relationship between the occurrence of great earthquakes and tectonic structures. Bull. Earthq. Res. Ins., Tokyo Univ., 47, 429-451.

Mohler, A.S. 1980. Earthquake/earth tide correlation and other features of the Susanville, California, earthquake sequence of June-July, 1976. Bull. Seism. Soc. Am., 70, 1583-1593.

Moore, H.D. 1979. Mapping and classification of structural linears in the Laurentide Park area of Quebec based on Landsat images. Earth Physics Branch Open File No. 79-19, Gregory Geoscience Ltd., 16 pp.

Morner, N-A. 1978. Faulting, fracturing, and seismicity as functions of glacio-isostasy in Fennoscandia. Geology, 6, 41-45.

Morton, J.D., Lo, K.Y., and Belshaw, D.J. 1975. Rock performance considerations for shallow tunnels in bedded shales with high lateral stresses. Proceedings, 12th Canadian Rock Mechanics Symposium, Kingston, Ont.

Morton, J.D., Belshaw, D.J., and Palmer J.H.L. 1979. Results of instrumentation and observation of a tunnel in bedded rock with high residual (in situ) stresses. Proceedings, Rapid excavation and tunnelling conference, Atlanta, Georgia, June 18-21, p. 917-935.

Nichols, T.C. 1980. Rebound, its nature and effect on engineering works. Quat. J. Eng. Geol. London, 13, 133-152.

Niewiadomski, J. and Ritsema, A.R. 1980. The stress field induced by cracks and the occurrence of earthquakes. Geophysics, in Proceedings of the Koninklijke Nederlandse Akademie van Wetenshappen, Series B, 83, 361-377.

Nyland, E. 1973. An interpretation of vertical crustal movement observations in the area of Lac St-Jean, Quebec. Can. J. Earth Sci., 10, 1471-1478.

Oliver, J., Johnson, T. and Dorman, J. 1970. Postglacial faulting and seismicity in New York and Quebec. Can. J. Earth Sci., 7, 579-590.

Palmer, J.H.L., and Lo, K.Y., 1976. In situ measurements in some near-surface rock formations - Thorold, Ontario. Can. Geotech. J., 13, 1-7.

Peltier, W.R., Farrell, W.E. and Clark, J.A. 1978. Glacial isostasy and relative sea level: a global finite element model. Tectonophysics, 50, 81-110.

Pomeroy, P.W., Simpson, D.W. and Sbar, M.L. 1976. Earthquakes triggered by surface quarrying - The Wappingers Falls, New York sequence of June, 1974. Bull. Seism. Soc. Am., 66, 685-700.

Prest, V.K., 1970. Quaternary geology of Canada. In Geology and economic minerals of Canada, Geological survey of Canada Economic Geology Report 1, 667-764.

Price, N.J. 1974. The development of stress systems and fracture patterns in undeformed sediments. Proceedings of the Third Congress of the International Society for Rock Mechanics, Denver. In Advances in Rock Mechanics, 1, Part A. National Academy of Sciences, Washington, DC, 487-496.

Price, N.J. 1979. Fracture patterns and stresses in granites. Geoscience Canada, 6, 209-212.

Raleigh, C.B., Healy, J.H. and Bredehoeft, J.D. 1972. Faulting and crustal stress at Rangely, Colorado. In Flow and Fracture of Rocks, Geophysical monograph 16, 275-284.

Ranalli, G. and Chandler, T.E. 1975. The stress field in the upper crust as determined from in situ measurements. Geologische Rundschau, 64, 653-674.

Richardson, R.M., Solomon, S.C. and Sleep, N.H. 1979. Tectonic stress in the plates. Reviews of Geophys. and Space Phys., 17, 981-1019.

Saada, A.S. 1974. Elasticity - Theory and Applications. Pergamon Press Inc., New York, pp. 643.

Saull, V.A., and Williams, D.A., 1974. Evidence for recent deformation in the Montreal area. Can. J. of Earth Sci., 11, 1621-1624.

Sbar, M.L. and Sykes, L.R. 1973. Contemporary compressive stress and seismicity in eastern North America: An example of intra-plate tectonics. Geol. Soc. Am. Bull., 84, 1861-1882.

Sbar, M.L. and Sykes, L.R. 1977. Seismicity and lithospheric stress in New York and adjacent areas. J. Geophys. Res., 82, 5771-5786.

Scheidegger, A.E. 1977. Joints in Ontario, Canada. Rivista Italiana di Geofisica, Sci., 4, 1-10.

Scheidegger, A.E., 1979. The enigma of jointing. Rivista Italiana di Geofisica, 5, 1-4.

Scheidegger, A.E., 1980a. Alpine joints and valleys in the light of the neotectonic stress field. Rock Mechanics, Suppl. 9, 109-124.

Scheidegger, A.E. 1980b. The orientation of valley trends in Ontario. Zeit. fur Geomorphologie, 24, 19-30.

Simmons, G., Tillson, D., Murphy, V., Leblanc, G., Doherty, J., Sharp, J., Klimkiewicz, G., Wang, H., Illfelder, H., and Roeloff, E. 1978. Gravity, stress, and earthquakes in Washington State and surrounding areas (abstract). 3rd International Conference on Basement Tectonics, 15-19 May 1978, Fort Lewis College, Durango, Colorado.

Skinner, B.J., 1966. Thermal expansion. In Handbook of Physical Constants, edited by S.P. Clark, Geological Soc. of Am., Memoir 97, 75-96.

Stein, S., Sleep, N.H., Geller, R.J., Wang, S.-C. and Kroeger, G.C. 1979. Earthquakes along the passive margin of eastern Canada. Geophys. Res. Letters, 6, 537-540.

Stevens, A.E. 1980. Reexamination of some larger La Malbaie, Quebec, earthquakes (1924-1978). Bull. Seism. Soc. Am., 70, 529-557.

Strangway, D.W. 1980. Geophysical methods and toxic waste disposal. Geoscience Canada, 7, 30-32.

Sykes, L.R. and Sbar, M.L. 1974. Focal mechanism solution of intraplate earthquakes and stresses in the lithosphere. In Geodynamics of Iceland and the North Atlantic Area, edited by L. Kristjansson, D. Reidel, Boston, Mass., 207-224.

Tammemagi, H.Y. 1979. Developing the data for nuclear waste disposal. Geoscience Canada, 6, 205-208.

Taylor, A. and Judge, A. 1979. Permafrost studies in northern Quebec. Geogr. Phys. Quat., 33, 245-251.

Turcotte, D.L. and Oxburgh, E.R. 1976. Stress accumulation in the lithosphere. Tectonophysics, 35, 183-199.

Vanicek, P. 1976. Contemporary vertical crustal movements in southern Ontario. Prepared for Earth Physics Branch, E.M.R. Dept. of Surveying Engineering, Univ. New Brunswick, Technical Report 39.

Vanicek, P. and Hamilton, A.C. 1972. Further analysis of vertical crustal movement observations in the Lac St. Jean area, Quebec. Can. J. Earth Sci., 9, 1139-1147.

Walcott, R.I. 1970. Isostatic response to loading of the crust in Canada. Can. J. Earth Sci., 7, 716-727.

Walcott, R.I. 1972. Late Quaternary vertical movements in eastern North America: Quantitative evidence of glacio-isostatic rebound. Rev. of Geophys. and Space Phys., 10, 849-884.

Walcott, R.I. 1977. Rheological models and observational data of glacio-isostatic rebound. In Earth rheology, isostacy and eustacy, ed. Morner, N.-A., John Wiley and Sons, Chichester, U.K., 3-10.

Weiss, M. 1977. Stress in the earth. (ed) Pure and applied geophysics, v. 115. Birkhauser Verlag Basel and Stuttgart, pp. 458.

Wesnousky, S.G. and Scholz, C.H. 1979. Shield drag: A possible contributor to the intraplate stress field. EOS, 60, 955.

Wesnousky, S.G. and Scholz, C.H. 1980. The craton: Its effect on the distribution of seismicity and stress in North America. Earth and Planetary Science Letters, 48, 348-355.

Wetmiller, R.J. 1975. The Quebec-Maine border earthquake, 15 June 1973. Can. J. Earth Sci., 12, 1917-1928.

Wetmiller, R.J., 1980. Investigation of earthquakes in Burlington, Ontario. Seismological Service of Canada Internal Report 80-5, Earth Physics Branch, Ottawa, pp. 18.

Wetmiller, R.J. and Forsyth, D.A. 1981. Review of seismicity and other geophysical data around Nares Strait. Meddelser om Gronland, Geoscience (in press).

White, O.L., Karrow, P.F. and Macdonald, J.R. 1973. Residual stress relief phenomena in southern Ontario. Proc. of the 9th Canadian Rock Mechanics Symposium, Montreal, December 1973, 323-348.

Whitham, K. 1979. Extended abstract, Earthquake prediction research in eastern Canada. Physics of the Earth and Planetary Interiors, 18, 339-340.

Wilson, A.W.G. 1902. Some recent folds in the Lorraine Shales. Canadian Record of Science, 8 (8), 525-531.

Winder, C.G., 1955, Campbellford Map-area, Ontario. Geological Survey of Canada, paper 54-17, pp. 12 + map.

Yang, J.-P. and Aggarwal, Y.P. 1981. Seismotectonics of northeastern United States and adjacent Canada. J. Geophys. Res. (in press).

Zoback, M.L. and Zoback, M. 1980. State of stress in the conterminous United States. J. Geophys. Res., 85, 6113-6156.

Table 1

Eastern and northeastern Canada earthquakes with P-wave nodal solutions**

Date	Origin Time	Lat.	Lon.	Depth (km)	m_b	M_s	Reference
Nov. 20/33	23:21:32	73.3°N	70.7°W	65	-	7.3	Stein et al. (1979)
Sept. 04/63	13:32:12	71.4°N	73.3°W	7	5.9	6.2	Stein et al. (1979)
Nov. 24/69	21:14:13	60.5°N	58.7°W	33+	5.0	-	Sykes and Sbar (1974)
Dec. 12/70	11:03:10	68.4°N	67.3°W	9	4.9	-	Hashizume (1973)
Oct. 02/71	03:19:28	64.4°N	86.5°W	21	5.0	-	Hashizume (1974)
Dec. 07/71	12:04:19	55.0°N	54.3°W	16	5.4	5.3	Hashizume (1977)
Jan. 21/72	14:43:42	71.9°N	74.7°W	6	4.5	-	Hashizume (1973)
June 15/73	01:09:05	45.39°N	71.02°W	6	4.9#	-	Wetmiller (1975) Herrmann (1979)
July 12/75	12:37	46.5°N	76.3°W	17	4.2	-	Horner et al. (1978)
Nov. 12/76	14:47:25	72.5°N	70.2°W	33+	5.4	5.1	Stein et al. (1979)
Feb. 18/78	14:48	46.3°N	74.1°W	7	4.1#	-	Horner et al. (1979)
Aug. 19/79	22:49:31	47.7°N	69.9°W	10	5.0#	-	Hasegawa and Wetmiller (1980)

** microearthquakes near La Malbaie, Quebec (Leblanc and Buchbinder, 1977) not included

+ normal depth assumed

m_bL_g

TABLE 2. STRESS MEASUREMENTS AND STRESS DIRECTIONS FROM SURFICIAL FEATURES

Feature	Locality	Lat. ° N.	Long. ° W.	Lithology	Principal Stress P=Major	Horizontal (MPa) Q=Minor	Inferred Compression Direction	Comments	References
A. STRESS MEASUREMENTS AT SHALLOW DEPTH									
Borehole	Thorold	43.1	79.2	Limestone	6.6-14.7	5.2-12.1	060	12 - 25 m deep	Palmer & Lo (1976)
Borehole	Mississauga (Lakeview)	43.6	79.5	Shale	6.9	-	?NNE	10 - 15 m deep	Lo & Morton (1976); Lo (1978); Morton et al. (1975)
Borehole	Pickering (W. Duffin)	43.8	79.1	Shale	4.4-7.4	3.1-6.6	019	18 - 24 m deep	Morton et al. (1979)
Borehole	Wesleyville	44.0	78.3	Limestone	9.8-13.4	5.4-10.3	165	37 m deep	Lo (1978)
Borehole	Niagara Falls	43.1	79.1	Shale	10	-	-	35 m deep	Lo (1978)
Borehole	Témiscaming	46.7	79.1	Gneiss	20	7.6	105	60 m deep	Comm. Hydro-Québec
Borehole	Darlington	43.9	78.7	Limestone	13	8.5	067	45 - 208m deep	Haimson (1978)
Surface	Ottawa	45.4	75.7	Limestone	1/2(P+Q)	= 2.8	-	Surface	Grant in Herget (1980)
Surface	North Bay	46.3	79.5	Granite	1/2(P+Q)	= 7.6	-	Surface	Grant in Herget (1980)
Borehole	Scarborough	43.8	79.2	Shale	1.7	1.6	090	70 m deep	Franklin & Hungr (1978)
Borehole	Niagara Falls	43.1	79.1	Dolomite	1.7-11.7	-1.9-1.9	044	2 - 7 m deep	Sellers in Franklin & Hungr (1978)
Borehole	Mississauga (Heart Lake)	43.6	79.7	Shale	1.5-9.5	1-6	?E-W	15 m deep	Lo et al. (1979)

Feature	Locality	Lat. ° N.	Long. ° W.	Lithology	Length (m)	Strike	Inferred Compression Direction	Comments	References
B. HISTORIC FOLDS, QUARRY-FLOOR BUCKLES AND SQUEEZE PHENOMENA									
Fold	Westover	43.3	80.1	-	200	-	-	in 1949	Karrow (1963)
Buckles (4)	Milton	43.5	79.9	Limestone	70	NE	135	Same quarry	White et al. (1973)
Buckles (2)	Milton	43.5	79.9	Limestone	-	SE	045	Same quarry	White et al. (1973)
Buckle	Marmora	44.5	77.7	Limestone	100	SE	045		Lo (1978); Coates (1964)
Buckle	Terrebonne	45.7	73.6	Limestone	100	NNW	060		Saull & Williams (1974)
Buckle	Terrebonne	45.7	73.6	Limestone	40	NNW	060		Saull & Williams (1974)
Buckle	St Eustache	45.6	73.9	Dolomite	30	NW	045	Same Quarry	Saull & Williams (1974)
Buckle	St Eustache	45.6	73.9	Dolomite	45	E-W	000	Same Quarry	Saull & Williams (1974)
Squeeze	Niagara	43.1	79.1	Limestone	-	N-S	-	Power Canal	Lo (1978)
Squeeze	Niagara	43.1	79.1	Limestone	-	NNE	-	Power Canal	Lo (1978)
Squeeze	Hamilton	43.3	79.9	Dolomite	-	NW	-	Sewer Trench	Roegiers et al. (1979)

Table 2 continued

Feature	Locality	Lat. ° N.	Long. ° W.	Lithology	Length (m)	Strike	Dip	Inferred Compression Direction	Comments	References
C. POSTGLACIAL THRUST FAULTS IN ONTARIO AND WESTERN QUEBEC										
Faults (6)	Haileybury	47.45	79.74	Slate	3	060	80°NW	150	17 mm throw	Adams, 1980, unpub.
Faults (7)	Larder Lake	48.12	79.68	Slate	2	110	80°S	020	21 mm throw	" " "
Faults (5)	Duparquet	48.52	79.22	Schist	2	070	90°	160	5 mm throw	" " "
Fault	Arntfield	48.20	79.26	-	-	156	-	066	40 mm throw	Johnson, 1969, unpub.
Fault	Rouyn-Noranda	48.26	79.04	-	-	093	-	003	6 mm throw	" "
Fault	Rouyn-Noranda	48.26	79.07	-	-	089	-	179	12 mm throw	" "
Faults (2)	Beardmore	49.5	88	Slate	-	093	-	003	12 mm throw	Oliver et al. (1970)
Fault	Flanders	49	92	Slate	-	086	-	176	6 mm throw	"
Faults (24)	Banning	49	92	Slate	20	080	65°N	170	550 mm throw	Lawson (1911)
Fault	Longlac	50	87	Slate	-	159	90°	069	19 mm throw	Oliver et al. (1970)
Fault	Longlac	50	87	Slate	-	049	90°	139	13 mm throw	"
Fault	Shebandowen	49	90	Slate	-	102	-	012	6 mm throw	"
Fault	Shebandowen	49	90	Slate	-	098	-	008	13 mm throw	"
D. FOLDS OF PROBABLE POSTGLACIAL AGE IN SOUTHERN ONTARIO										
Fold	Mississauga	43.4	79.6	Shale	-	N10°W	-	080	1 m high	Wilson (1902)
Fold	Tullamore	43.8	79.8	Shale	500	N70°E	-	160	1 m high	White et al. (1973)
Fold	Burlington	43.3	79.8	Shale	2100	N84°W	-	006	1 m high	White et al. (1973); Karrow (1963)
Fold	Youngs Point	44.48	78.26	Limestone	1500	SE	-	045	2 m high	Lo (1978); Carson (1981)
Fold	Woodview	44.61	78.13	Limestone	100	NE	-	135	1 m high	Carson (1981)
Fold	Wellman	44.33	77.63	Limestone	1000	065	-	155	4 m high	Winder (1955); Carson (1981)

Table 2 continued

Feature	Locality	Lat. ° N.	Long. ° W.	Lithology	Length (m)	Strike	Dip	Inferred Compression Direction	Comments	References
E. BASEMENT FOLDS AND THRUST FAULTS OF UNCERTAIN AGE										
Fold	Oakville	43.5	79.7	Shale	-	N80°W	-	010		White et al. (1973)
Fold	Woodbridge	45.5	79.7	Shale	-	N52°W	-	038		White et al. (1973)
Fold	Joshua Creek, Oakville	43.5	79.7	Siltstone	-	N20°W	-	070		White et al. (1973)
Fold	Hull	45.4	75.7	Limestone	-	N25°W	-	065		Adams, 1980, unpub.
Fold	Acton	43.6	80.0	-	-	N30°E	-	120		Caley (1941)
Fold	Troy	43.3	80.2	-	-	N50°E	-	150		Caley (1941)
Fold	Rouge River	43.8	79.2	Shale	-	120°	-	030	pre-last glacial	Bowlby, 1981 pers. comm.
Fold	Montreal	45.5	73.6	Limestone	-	065	-	155	probably ice thrust	Durand & Ballivy (1974)
Fold	Camden East	44.3	76.8	-	-	-	-	115		Bowlby, 1981 pers. comm.
Fold	Warsaw	44.4	78.1	-	-	-	-	090	faulted fold	Carson (1981); Bowlby, 1981 pers. comm.
Fault	Oakville	43.5	79.7	Siltstone	-	N20°W	54°NW	150		White et al. (1973)
Fault	Oakville	43.5	79.7	Shale	-	NW	70°SW	045		White et al. (1973)
Fault	Claireville	43.7	79.6	Shale	-	N-S	17°W	090	0.3 m slip	White et al. (1973)
Fault	Zimmerman	43.4	79.8	Siltstone	-	N-S	30°E	090	0.6 m slip	White et al. (1973)
F. STRESS DIRECTIONS FROM JOINT ORIENTATIONS IN SOUTHERN ONTARIO										
									Tension axis =	
Joints	Amherstburg	42.1	83.1	Limestone	-	258;001*	-	132	042°	Scheidegger (1980b)
Joints	Niagara Falls	43.1	79.1	Limestone	-	248;009	-	120	030	Scheidegger (1980b)
Joints	Hamilton	43.2	79.9	Limestone	-	254;342	-	028	118	Scheidegger (1980b)
Joints	Toronto	43.7	79.4	Shale	-	069;344	-	116	026	Scheidegger (1980b)
Joints	Bancroft	45.0	77.9	Metasediments	-	261;181	-	131	041	Scheidegger (1980b)
Joints	Three-Mile-Lake	45.2	79.4	Gneiss	-	031;303	-	077	167	Scheidegger (1980b)
Joints	Parry Sound	45.4	80.0	Diorite	-	190;138	-	074	164	Scheidegger (1980b)
Joints	Sudbury-Espanola	46.5	81.5	Metasediments	-	267;190	-	139	048	Scheidegger (1980b)
Joints	Elliot Lake	46.4	82.7	Metasediments	-	250;177	-	123	034	Scheidegger (1980b)

* Azimuth of the two joint sets (x;y).

Table 3

Summary of compression directions derived from near surface measurements and surficial features in eastern Canada

	Source	N*	R+	Compression direction: Mean#	Compression direction: Standard deviation#
Stress measurements	Table 2A	9	0.43	064	18
Quarry-floor buckles	Table 2B	7	0.53	045	16
Postglacial faults	Table 2C	13	0.58	000	15
Pop-ups	Table 2D	6	0.28	-015	23
Bedrock folds and faults	Table 2E	14	0.16	084	27
Joints	Table 2F	9	0.82	133**	9

* N = Number of observations.

\+ R = Mean length of the resultant vector (1.00 = uniform direction).

\# Circular mean and standard deviation. Mean direction is degrees clockwise from north.

** Or 043° (May be 90° in error - see text).

Table 4

Selected values for Canadian Shield (for Fig. 14)

Parameter	Symbol	Value	Reference
Average density			
overburden	$\bar{\rho}$	2.7 Mg/m^3	
upper mantle	ρ_m	3.2 Mg/m^3	
Poisson's ratio	ν	0.25	
Linear coefficient of thermal expansion	α_L	$8 \times 10^{-6}/°C$	Skinner (1966)
Young's Modulus	E	8×10^{10} N/m^2	
Thermal conductivity	k	2.5 W/mK	A.M. Jessop (personal commun. 1980)
Mantle contribution to heat flow	Q_m	28 mW/m^2	Jessop and Lewis (1978)
Crust contribution to heat flow	Q_c	12 mW/m^2	Jessop and Lewis (1978)
Postglacial heating	ΔT	4 C°	Taylor and Judge (1979)
Scale depth	b	1400 m	Jessop and Lewis (1978)

FIGURE CAPTIONS

Figure 1. Epicentres and magnitudes of southeastern Canada earthquakes with tectonic provinces and prominent geological structures (from Basham et al., 1979).

Figure 2. (a) stress components on cubic element
(b) total stress ($\overline{\sigma}$) on inclined face of tetrahedron with normal ($\overline{n}$) and direction cosines (l_1, l_2, l_3).

Figure 3. (a) general case of shear failure with associated Coulomb-Mohr failure diagram
(b) fault geometry for P-wave nodal solutions and associated Coulomb-Mohr failure diagram
(c) realistic or typical case of shear failure. Symbols are as defined in text.

Figure 4. (a) dislocation in displacement with pair of arrows indicating relative motion between opposite faces of fault
(b) equivalent force (double couple) representation in unfaulted medium, orthogonal dashed lines represent directions parallel and orthogonal to actual plane of failure
(c) deviatoric stress vectors or principal axes of moment tensor with dot representing null vector; dashed lines are as described previously
(d) Mohr representation of principal stresses ($\sigma_1 > \sigma_2 > \sigma_3$) for case where $\sigma_1 - \sigma_2 = \sigma_2 - \sigma_3$
(e) Mohr representation of deviatoric stress vectors shown in part (c). Symbols are as described in text.

Figure 5. Orientation of maximum principal stress component and deviatoric compression vector in northeastern United States (after Sbar and Sykes, 1977).

Figure 6. Top part shows ratio of horizontal to vertical stress from overcoring in western Ontario (from Herget, 1980). Lower part shows correct relative sequence of ratios (σ_{Hmax}/σ_V and σ_{Hmin}/σ_V) as inferred from fault-plane solutions of two Canadian shield earthquakes; absolute value of ratios not known.

Figure 7. Orientation of maximum stress component in eastern and northeastern Canada. Solid dots in smaller circles are equal area net projections of maximum principal stress in lower hemisphere; (1 to 7) are from Herget (1980) and (10) from J. Levay (personal communication, 1980). Lines in smaller circle (8) just north of Lake Ontario represent stereographic projection of vertical fractures and indicate strike of maximum horizontal component (from Haimson, 1978). Pairs of converging arrows northeast of Lake Huron (9) (Commission Hydro-Electrique du Québec, 1967) and in Labrador (11) (Benson et al., 1970) are also from in-situ stress measurements. Pairs of outward pointing (deviatoric extension) and inward pointing (deviatoric compression) arrows are

from fault-plane solutions (lower-hemisphere, equal-area projection) of 11 earthquakes listed in Table 1; dark areas correspond to compressional P-wave first motions.

Figure 8. Shallow-depth stress measurement sites (line shows maximum horizontal stress direction), quarry-floor buckles (line shows inferred compression direction, not axis of buckle), and joint-indicated stress directions (arrows indicate preferred compression direction according to Scheidegger (1980b); see text), in southern Ontario and adjacent Quebec, taken from Table 2, A, B, and F.

Figure 9. Postglacial faults and pop-ups in eastern Canada. Modified from Figure 3 of Adams (1981), with addition of newly reported occurrences near Ontario-Quebec border (from Table 2C).

Figure 10. Summary diagram showing azimuth of maximum horizontal stress direction inferred from surficial features and measurements. These are not stereograms. Arrows on first four diagrams give mean compression data (Table 3). Note large scatter in all diagrams.

Figure 11. Top part shows plate tectonic boundary forces for North America plate and bottom part, associated horizontal principal stress patterns for North America plate (part of Model E 31 of Richardson et al., 1979). Outline of plate in solid line and outline of continent in dashed line.

Figure 12. Schematic diagrams of boundary forces that generate stress pattern shown in Figure 11. Symbols F_R, F_T and F_D stand for ridge force, tensional force along subduction zone and viscous drag force along base of plate, respectively. Geometry of viscous drag force shown in lower diagram (from Wesnousky and Scholz, 1979, 1980).

Figure 13. Vertical profile showing parallel deformation of eroded surface. Symbol ΔR_E, represents thickness of eroded surface, and ΔR_I, uplift due to isostatic compensation. Boundaries are constrained to fixed radial directions (after Haxby and Turcotte, 1976).

Figure 14a. Variation in horizontal stress with depth for Canadian shield. Resultant, $\Delta\sigma_R$ of Eq. (9), is sum of 3 stress components, $\Delta\sigma_E^D$ (erosion), $\Delta\sigma_c$ (associated cooling) and $\Delta\sigma_p$ (postglacial heating); f=o for this case. See Table 4 for selected values for Canadian shield that are input to Eq. (9).

Figure 14b. Deviatoric horizontal stress ($\Delta\sigma_R$) as function of depth of erosion (ΔR_E) for five values of f, the fraction of isostatic compensation achieved.

Figure 15. Schematic diagram of lithospheric flexural stress pattern induced by deglaciation (from Stein et al., 1979) applied to Baffin Island-Baffin Bay region.

Figure 16. Epicentres of earthquakes in eastern and northern Canada superimposed on free-air gravity anomaly field. North of 60°N latitude, earthquakes are shown for time interval 1965 to 1977. Larger dots denote magnitudes ≥ 3 (from Forsyth, 1981).

Figure 17. Schematic profile of lithospheric flexure due to ice load showing deviatoric horizontal stress pattern at shallow depth (after Walcott, 1970) for 2-km-thick ice load.

Figure 18. Coulomb Mohr failure for different modes of faulting:
(a) material near failure
(b) increase in pore pressure (ΔP) results in reduction in effective normal stress
(c) weakening of frictional characteristic of fault results in decrease ($\Delta\theta$) of coefficient of friction ($\tan\theta$)
(d) chemical weakening of material results in decrease (ΔS) of cohesive strength (S). Other symbols are as defined in text.

Figure 19. Schematic diagram showing relation between amount of overstress and time required to initiate failure (from Knopoff, 1964).

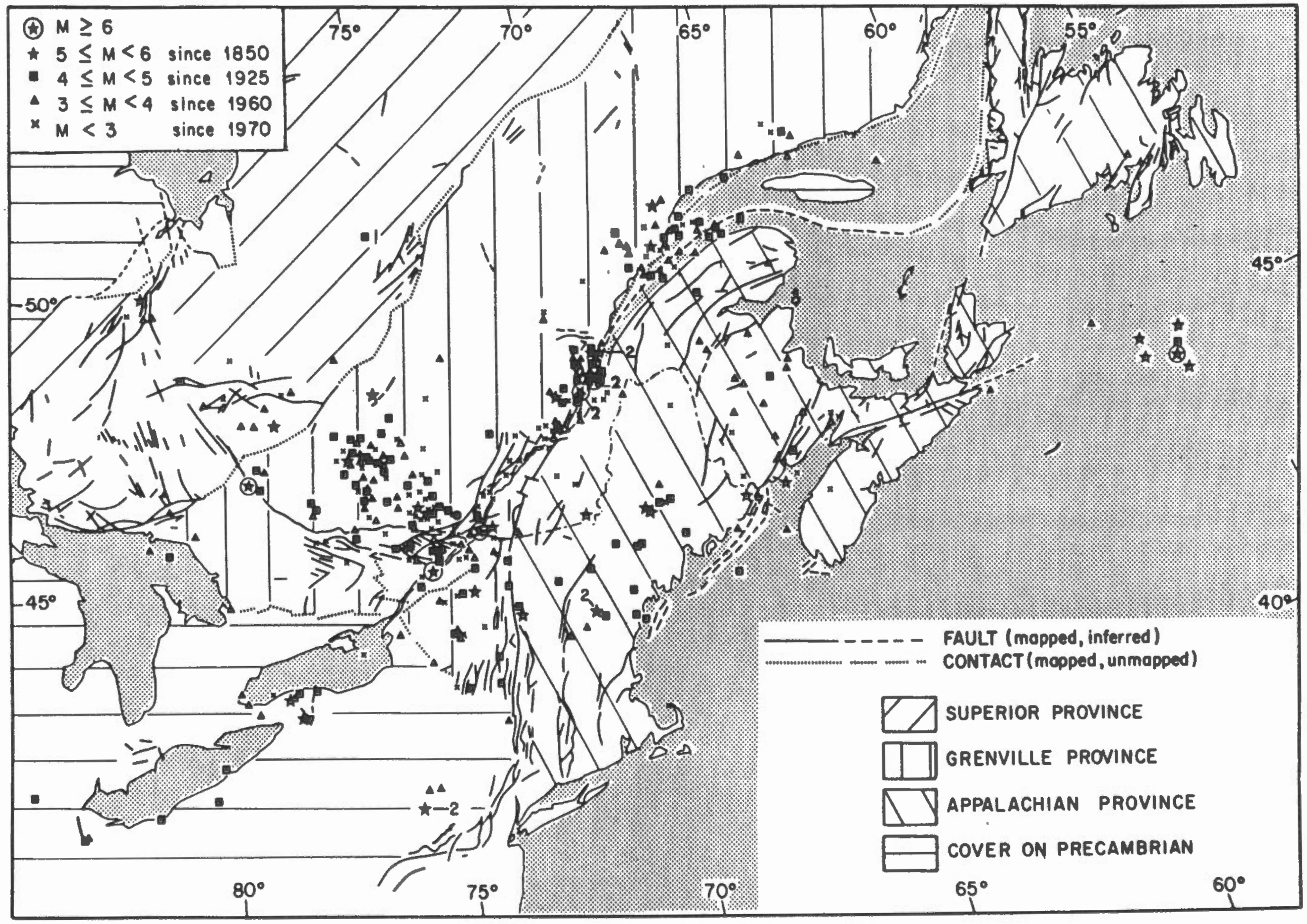
M ≥ 6
5 ≤ M < 6 since 1850
4 ≤ M < 5 since 1925
3 ≤ M < 4 since 1960
M < 3 since 1970
75°
70°
65°
60°
55°
50°
45°
40°
80°
75°
70°
65°
60°
FAULT (mapped, inferred)
CONTACT (mapped, unmapped)
SUPERIOR PROVINCE
GRENVILLE PROVINCE
APPALACHIAN PROVINCE
COVER ON PRECAMBRIAN

Figure 1.

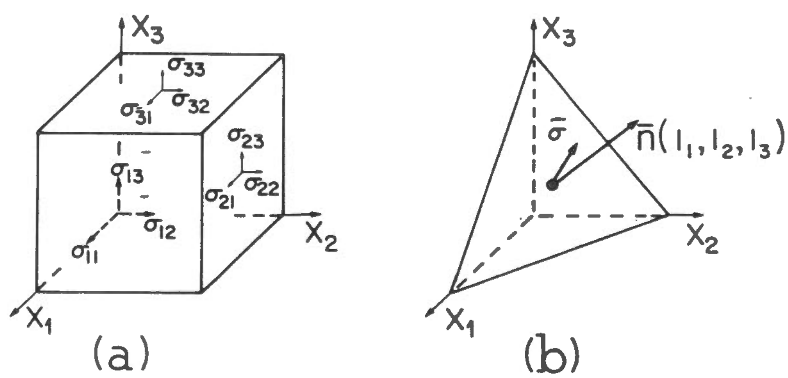

Figure 2.

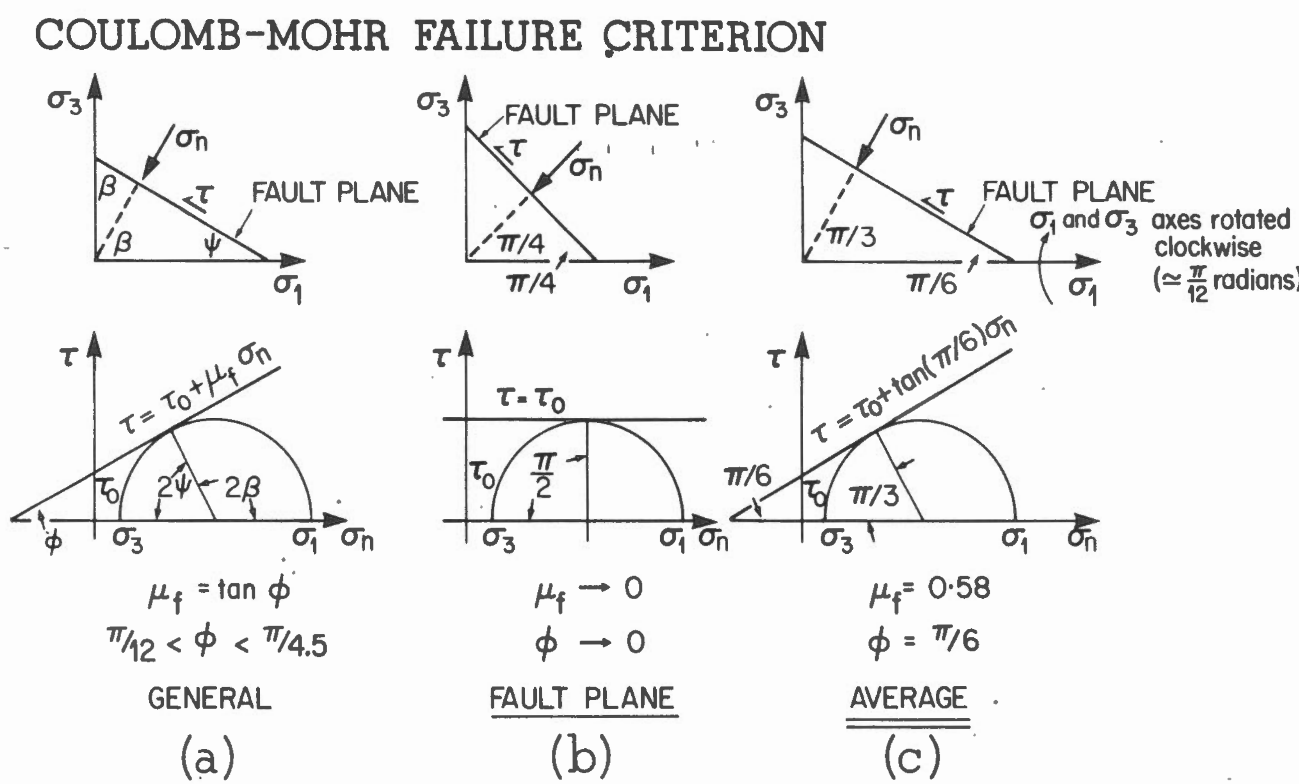
COULOMB-MOHR FAILURE CRITERION
σ3
σn
β
β
τ
FAULT PLANE
ψ
σ1
FAULT PLANE
τ
σn
π/4
π/4
σ1
σn
τ
FAULT PLANE
π/3
π/6
σ1
σ1 and σ3 axes rotated clockwise (≃ π/12 radians)
τ
τ = τ0 + μf σn
τ0
2ψ
2β
φ
σ3
σ1
σn
τ = τ0
τ0
π/2
τ = τ0 + tan(π/6)σn
π/6
π/3
μf = tan φ
π/12 < φ < π/4.5
GENERAL
(a)
μf → 0
φ → 0
FAULT PLANE
(b)
μf = 0·58
φ = π/6
AVERAGE
(c)

Figure 3.

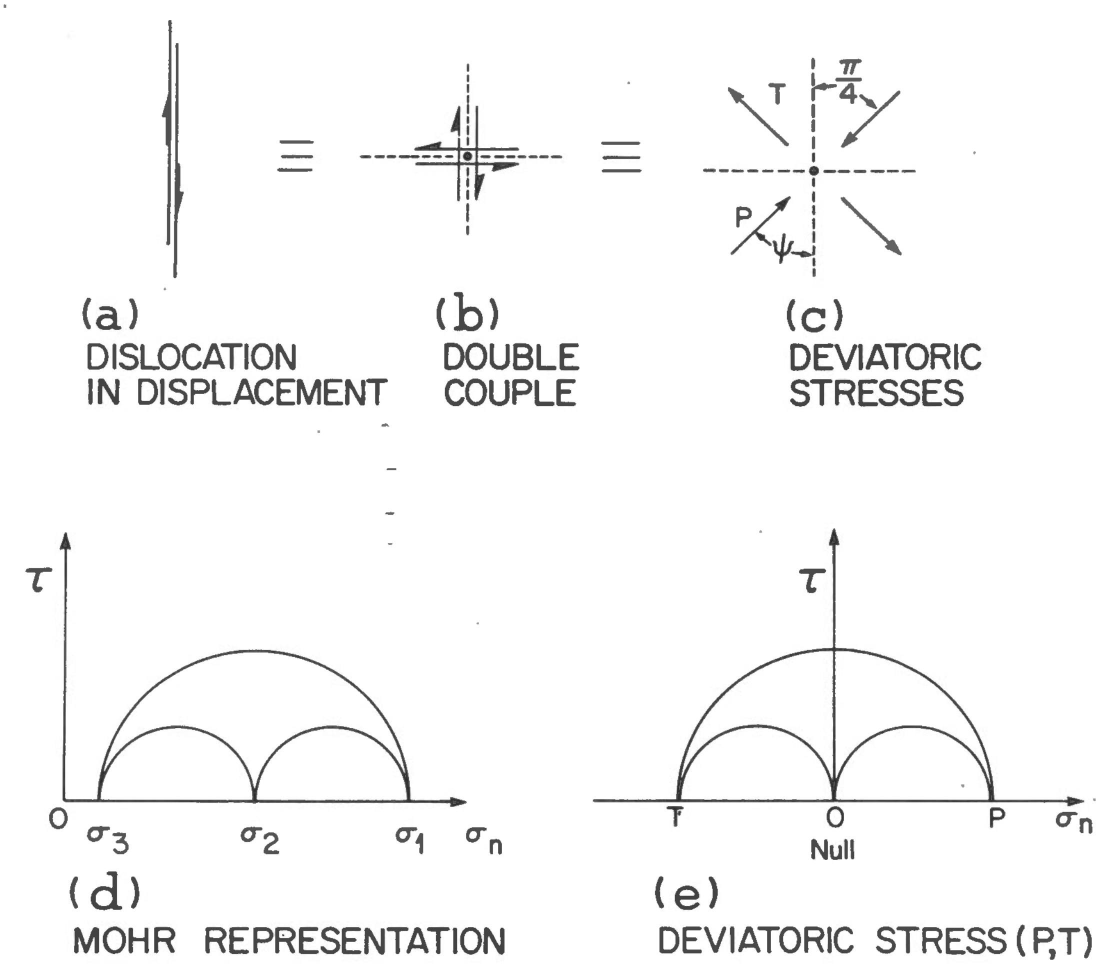
T
$\frac{\pi}{4}$
P
ψ
(a)
DISLOCATION
IN DISPLACEMENT
(b)
DOUBLE
COUPLE
(c)
DEVIATORIC
STRESSES
τ
O
σ_3
σ_2
σ_1
σ_n
(d)
MOHR REPRESENTATION
τ
T
O
Null
P
σ_n
(e)
DEVIATORIC STRESS (P,T)

Figure 4.

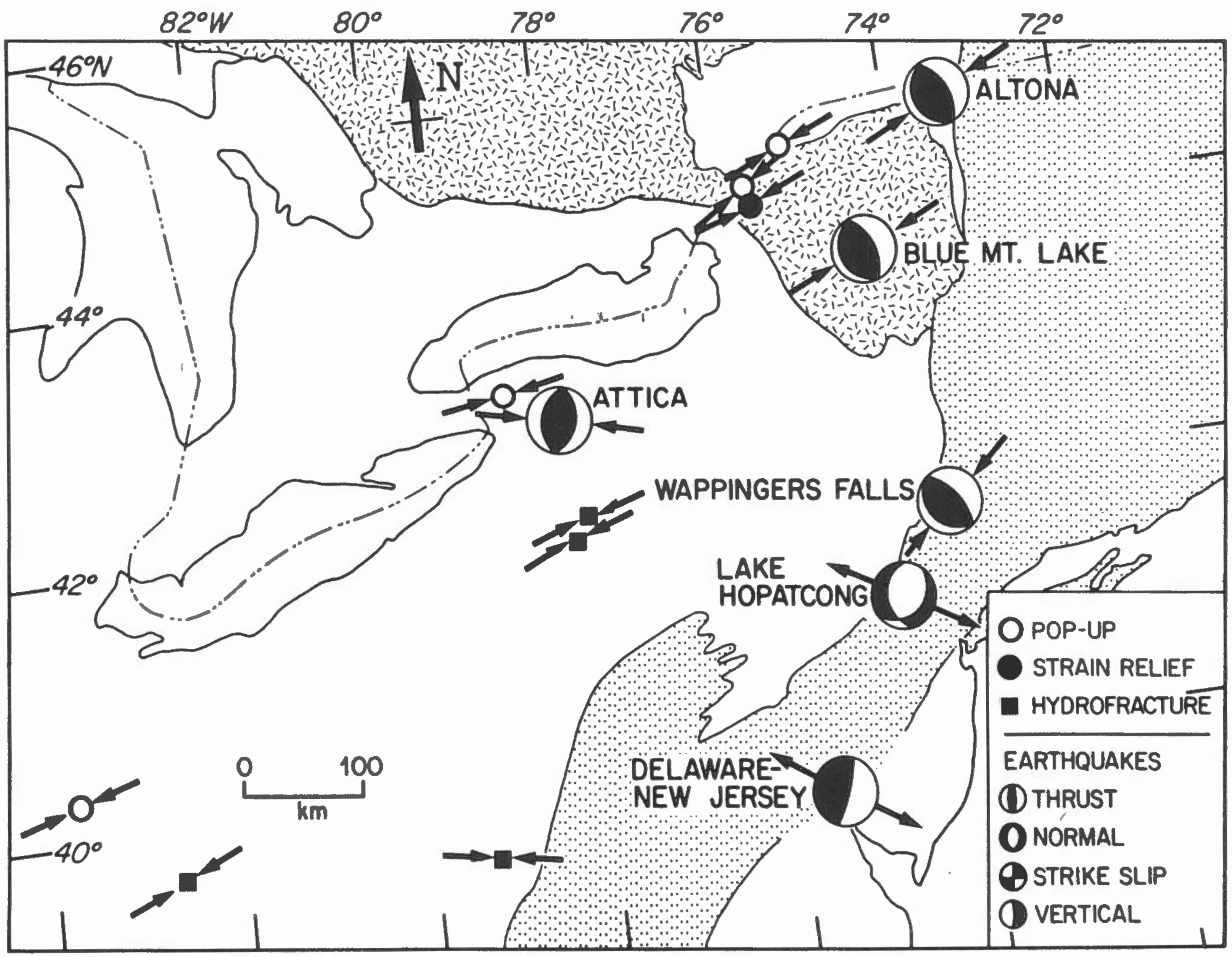
82°W
80°
78°
76°
74°
72°
46°N
44°
42°
40°
N
ALTONA
BLUE MT. LAKE
ATTICA
WAPPINGERS FALLS
LAKE
HOPATCONG
DELAWARE-
NEW JERSEY
0
100
km
POP-UP
STRAIN RELIEF
HYDROFRACTURE
EARTHQUAKES
THRUST
NORMAL
STRIKE SLIP
VERTICAL

Figure 5.

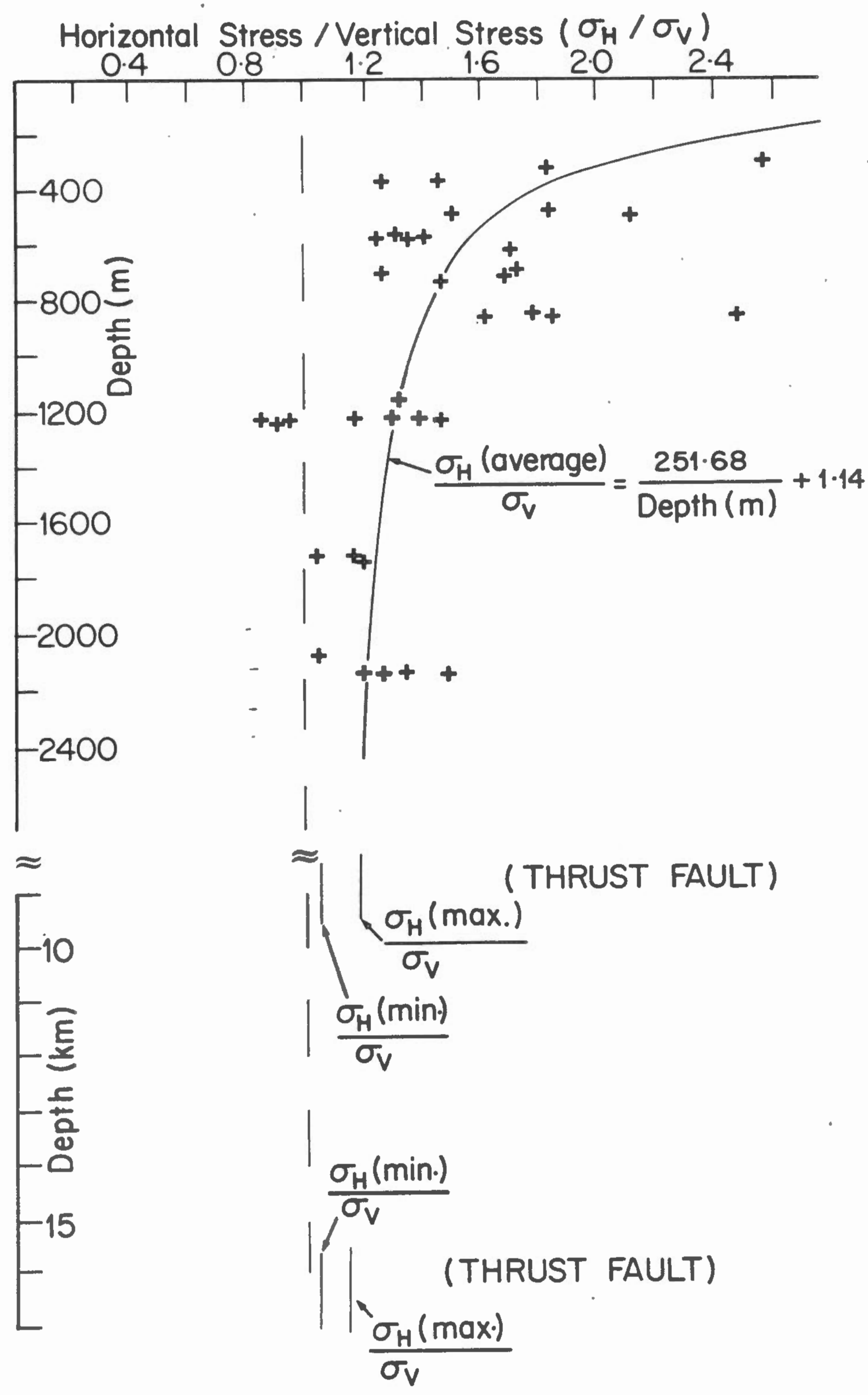

Horizontal Stress / Vertical Stress (σ_H / σ_V)
0·4
0·8
1·2
1·6
2·0
2·4
Depth (m)
400
800
1200
1600
2000
2400
$\frac{\sigma_H \text{ (average)}}{\sigma_V} = \frac{251{\cdot}68}{\text{Depth (m)}} + 1{\cdot}14$
(THRUST FAULT)
σ_H (max.) / σ_V
σ_H (min.) / σ_V
Depth (km)
10
15
σ_H (min.) / σ_V
(THRUST FAULT)
σ_H (max.) / σ_V

Figure 6.

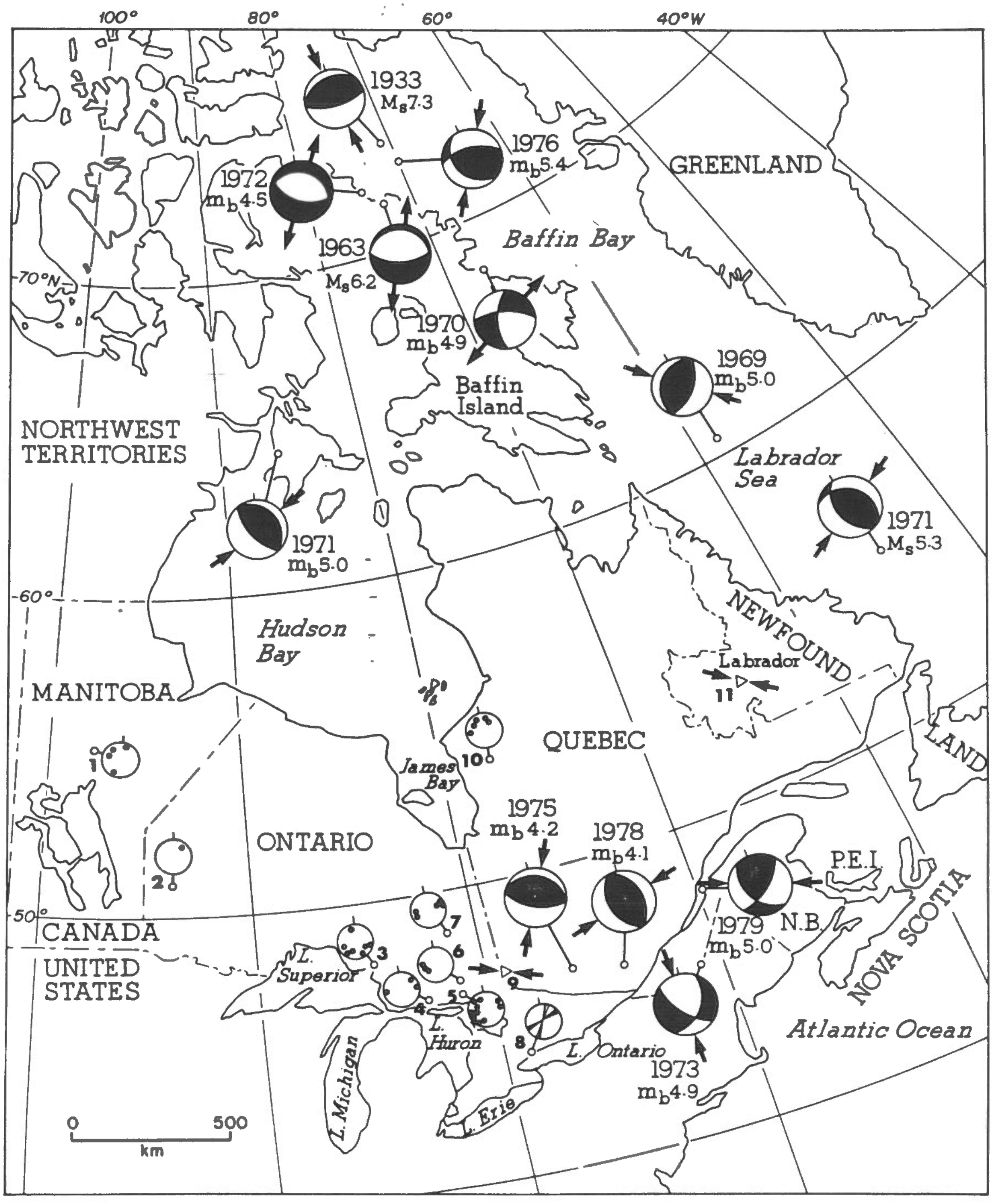
100°
80°
60°
40°W
70°N
60°
50°
1933
Ms7.3
1976
mb5.4
1972
mb4.5
1963
Ms6.2
GREENLAND
Baffin Bay
1970
mb4.9
1969
mb5.0
Baffin
Island
NORTHWEST
TERRITORIES
Labrador
Sea
1971
Ms5.3
1971
mb5.0
Hudson
Bay
NEWFOUND
Labrador
11
LAND
MANITOBA
QUEBEC
James
Bay
10
1
ONTARIO
1975
mb4.2
1978
mb4.1
2
P.E.I.
NOVA SCOTIA
CANADA
UNITED
STATES
1979
mb5.0
N.B.
7
3
6
L.
Superior
9
4
5
L.
Huron
8
L. Ontario
1973
mb4.9
Atlantic Ocean
L. Michigan
L. Erie
0
500
km

Figure 7.

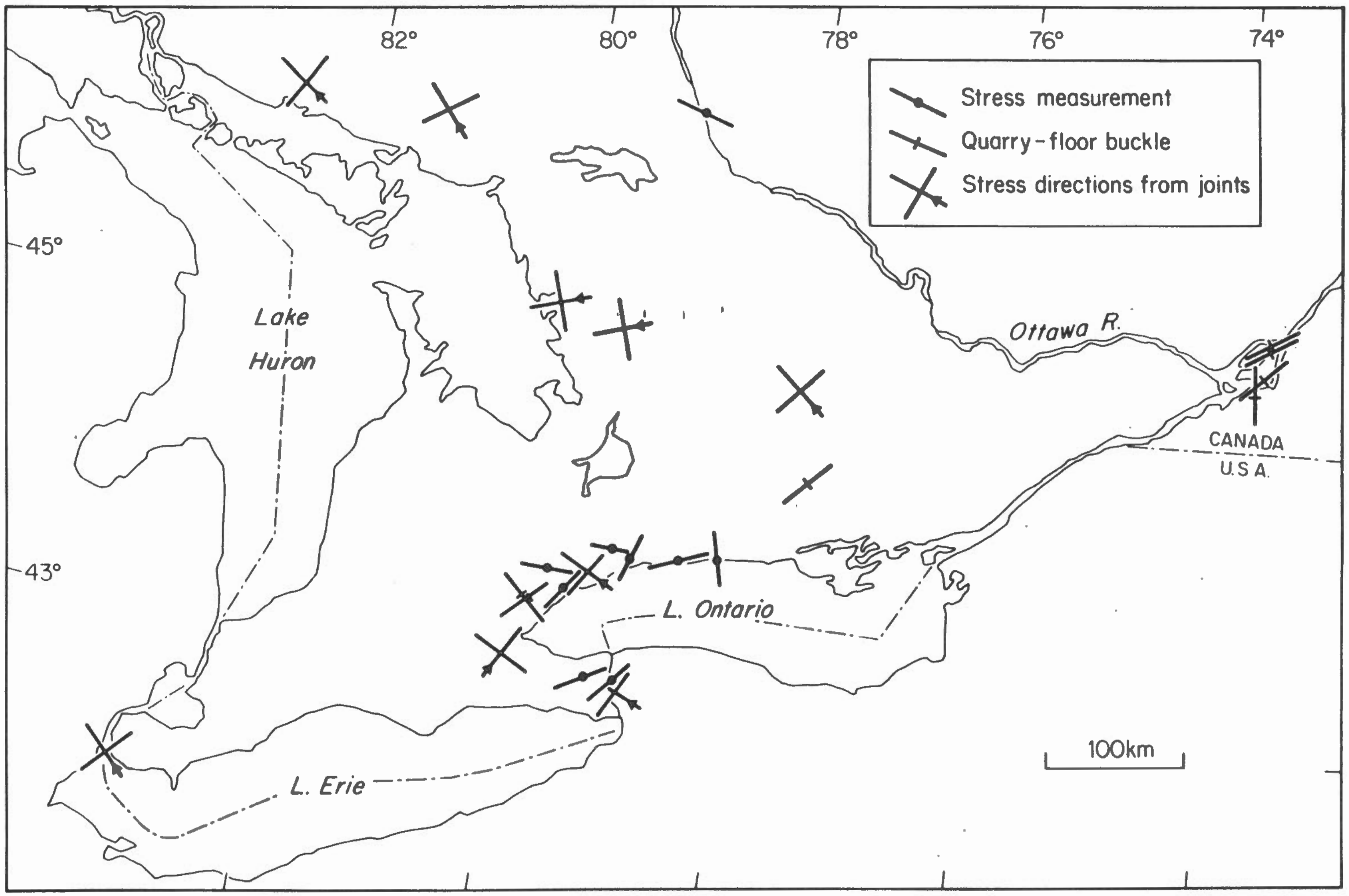
82°
80°
78°
76°
74°
45°
43°
Stress measurement
Quarry-floor buckle
Stress directions from joints
Lake
Huron
Ottawa R.
CANADA
U.S.A.
L. Ontario
L. Erie
100km

Figure 8.

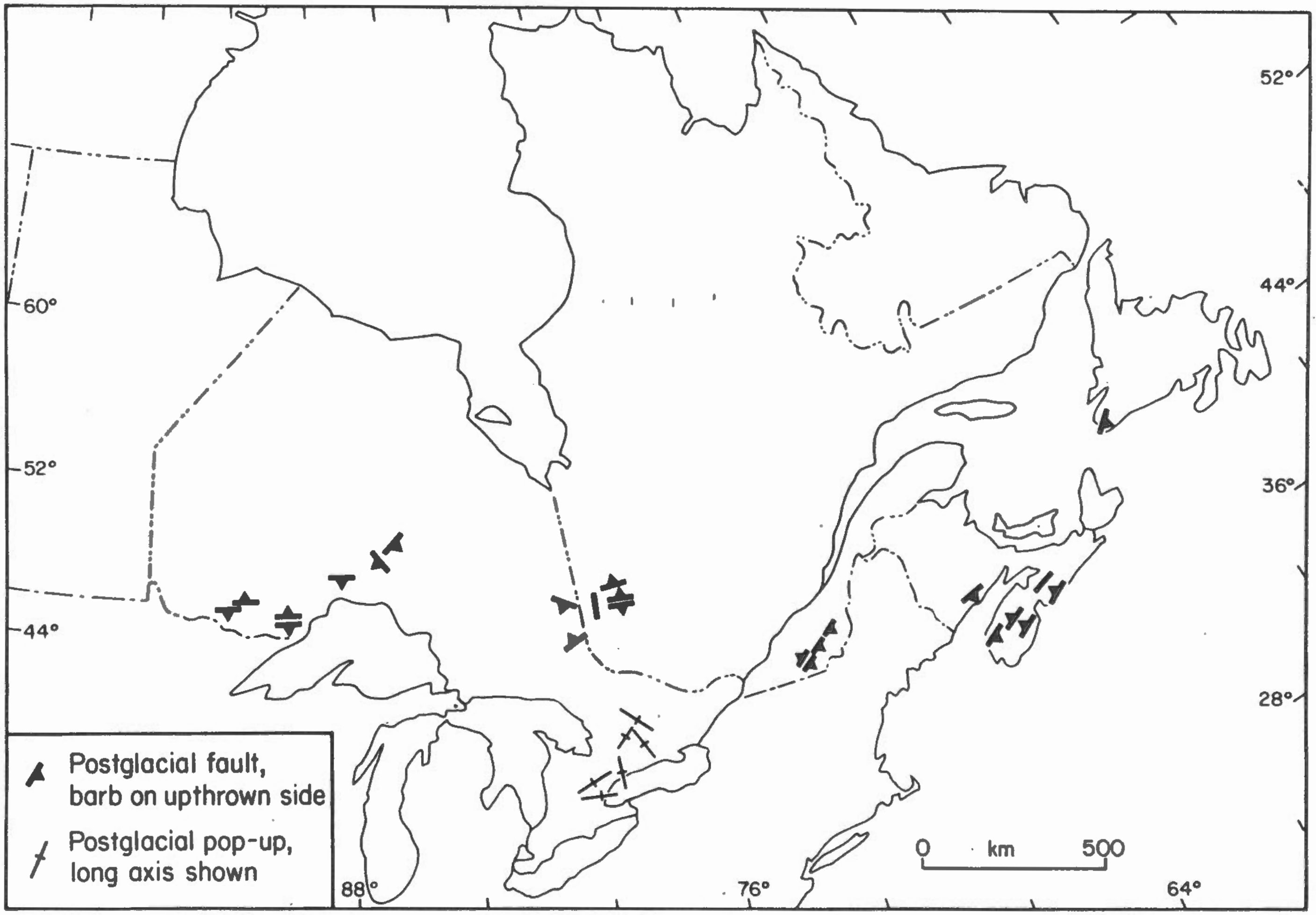
Postglacial fault,
barb on upthrown side
Postglacial pop-up,
long axis shown
0 km 500
52°
44°
36°
28°
60°
52°
44°
88°
76°
64°

Figure 9.

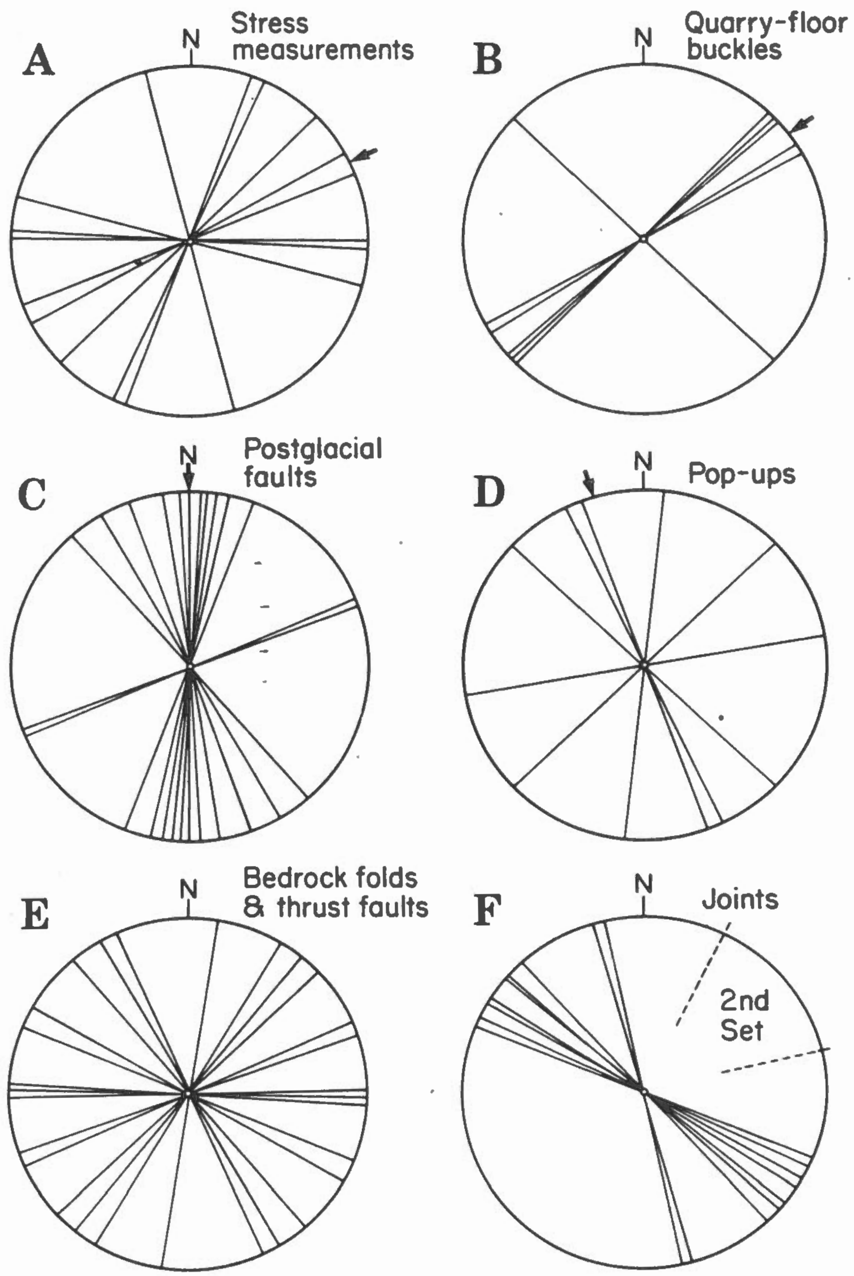

A
N
Stress measurements
B
N
Quarry-floor buckles
C
N
Postglacial faults
D
N
Pop-ups
E
N
Bedrock folds & thrust faults
F
N
Joints
2nd Set

Figure 10.

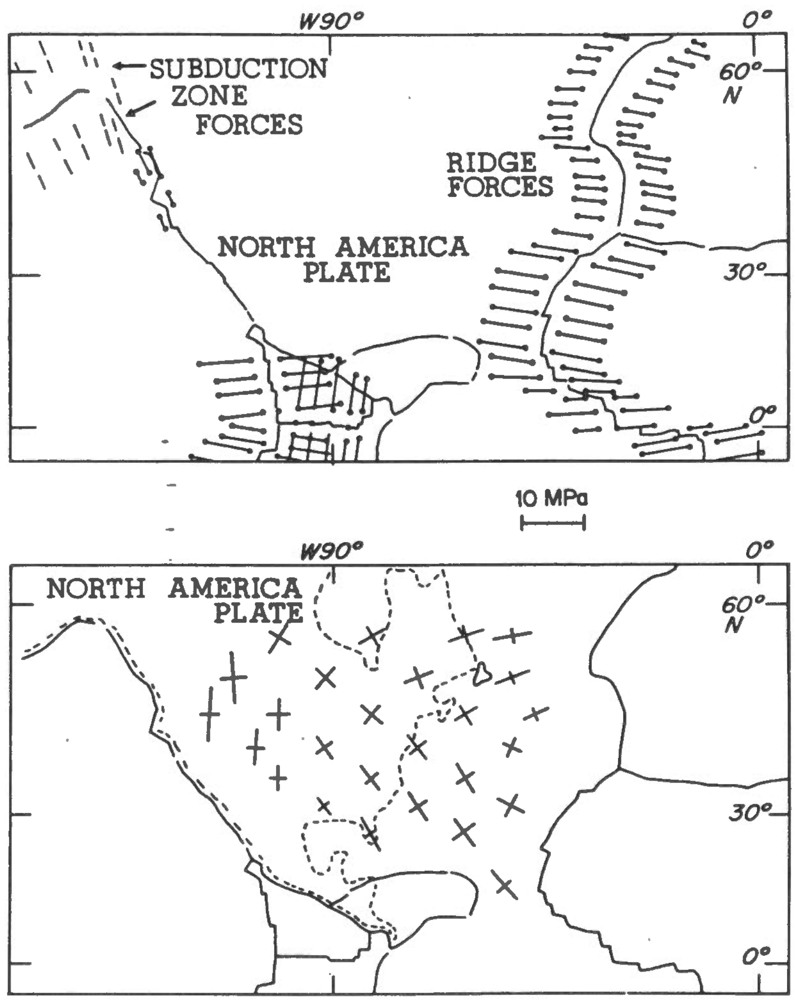
W90°
0°
SUBDUCTION
ZONE
FORCES
60°
N
RIDGE
FORCES
NORTH AMERICA
PLATE
30°
0°
10 MPa
W90°
0°
NORTH AMERICA
PLATE
60°
N
30°
0°

Figure 11.

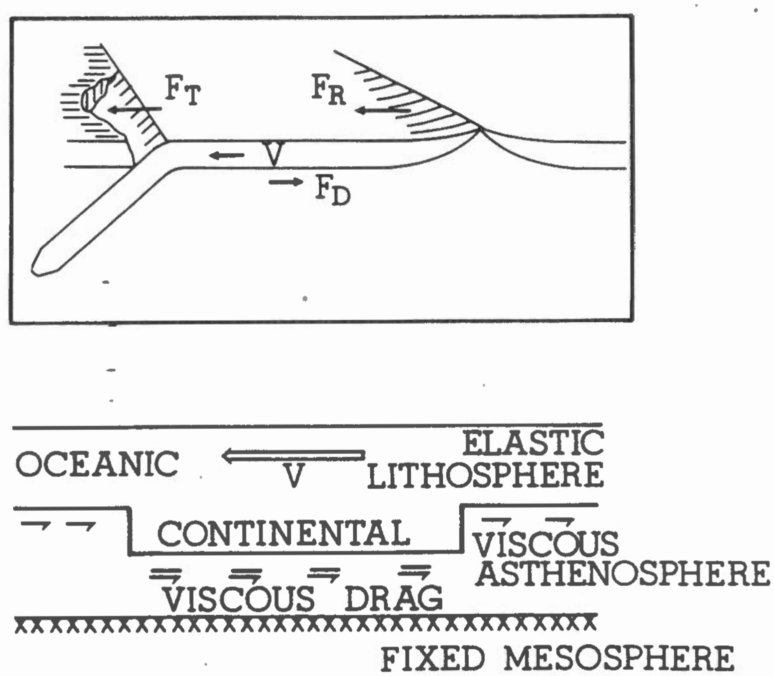
F_T
F_R
V
F_D
OCEANIC
V
ELASTIC
LITHOSPHERE
CONTINENTAL
VISCOUS
ASTHENOSPHERE
VISCOUS DRAG
FIXED MESOSPHERE

Figure 12.

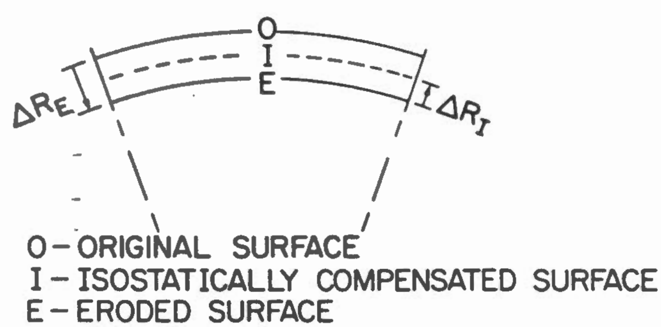
O
I
E
ΔR_E
ΔR_I
O - ORIGINAL SURFACE
I - ISOSTATICALLY COMPENSATED SURFACE
E - ERODED SURFACE

Figure 13.

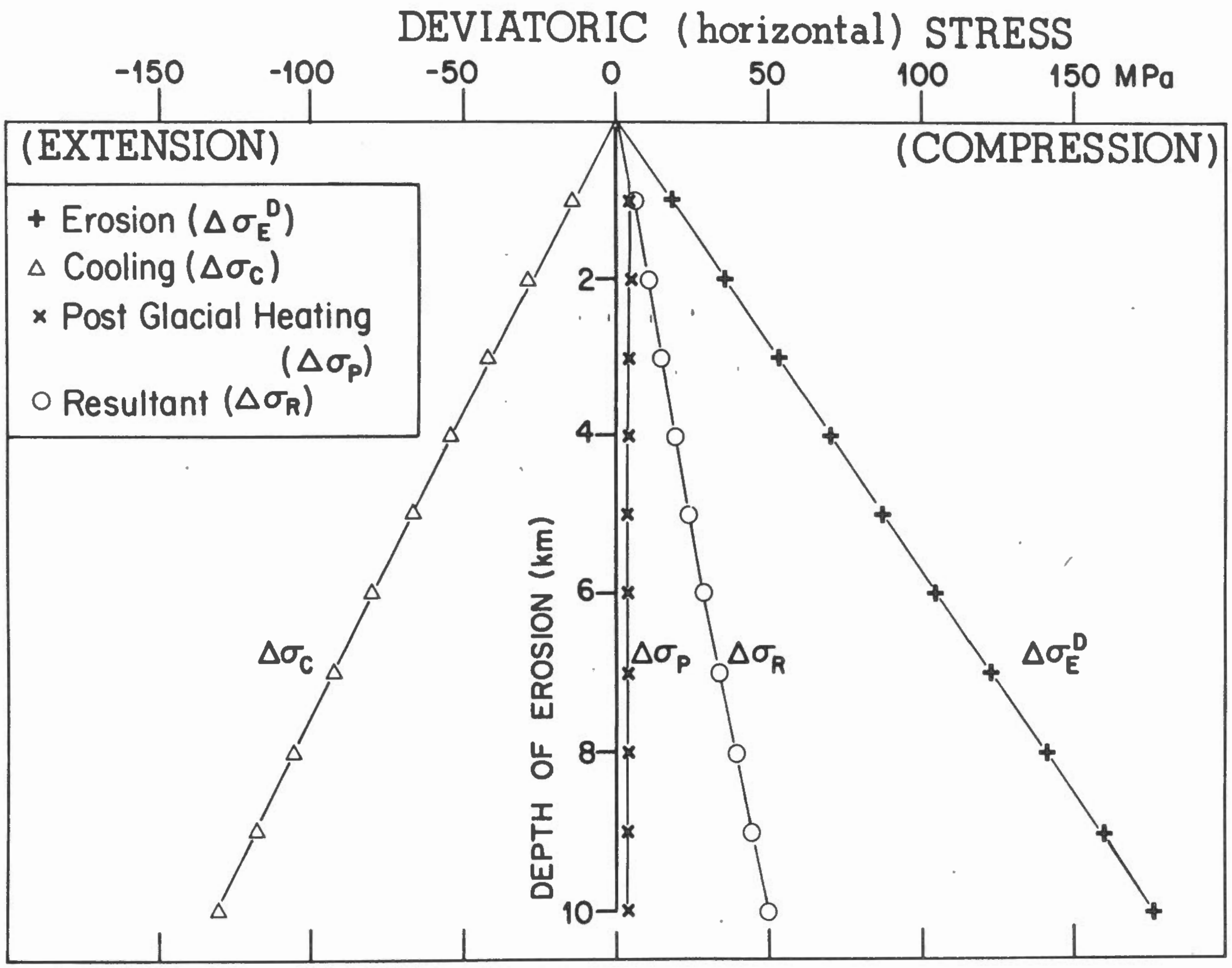
DEVIATORIC (horizontal) STRESS
-150
-100
-50
0
50
100
150 MPa
(EXTENSION)
(COMPRESSION)
+ Erosion ($\Delta\sigma_E^D$)
△ Cooling ($\Delta\sigma_C$)
× Post Glacial Heating ($\Delta\sigma_P$)
○ Resultant ($\Delta\sigma_R$)
DEPTH OF EROSION (km)
2
4
6
8
10
$\Delta\sigma_C$
$\Delta\sigma_P$
$\Delta\sigma_R$
$\Delta\sigma_E^D$

Figure 14a.

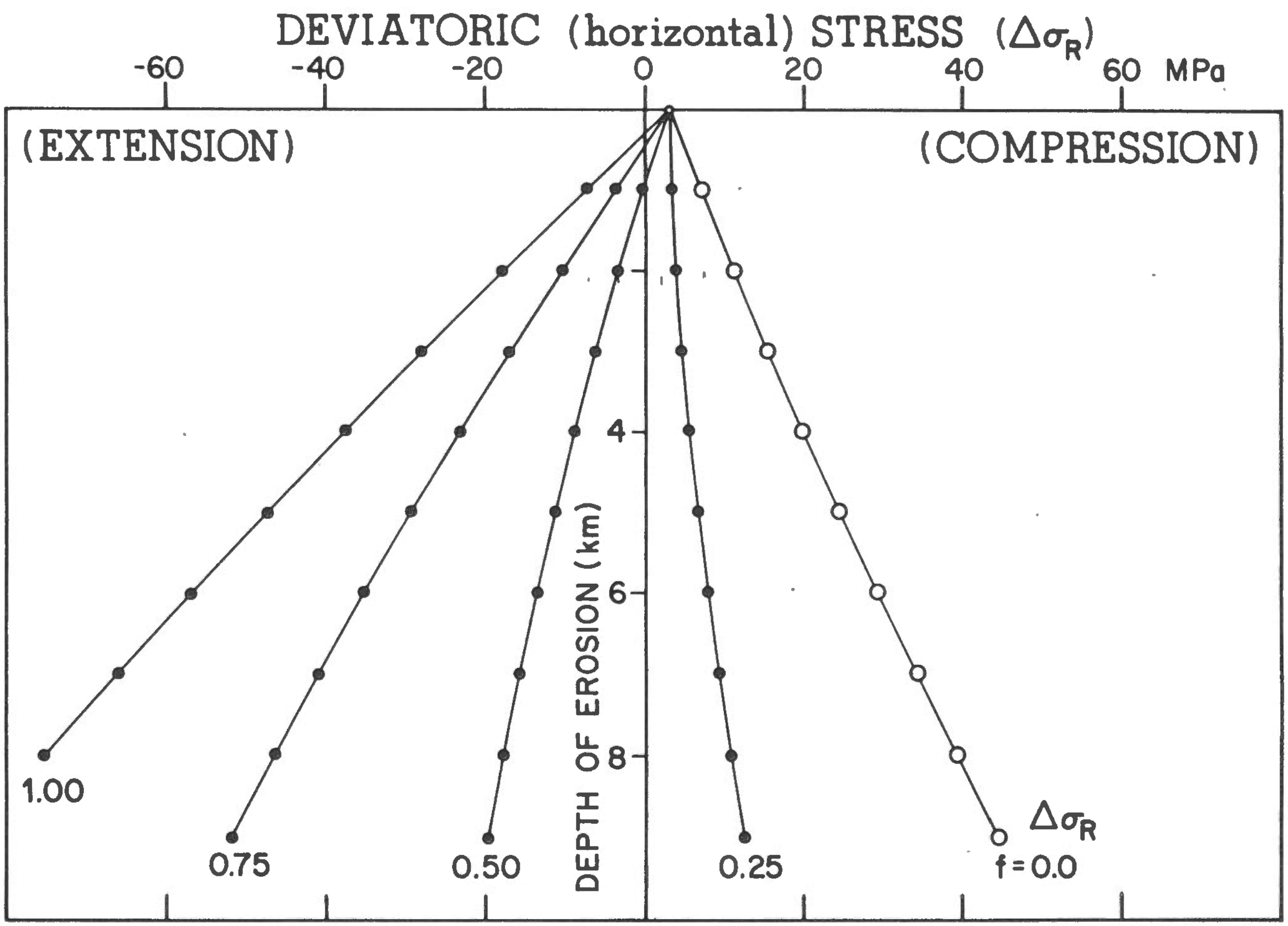

DEVIATORIC (horizontal) STRESS ($\Delta\sigma_R$)
-60
-40
-20
0
20
40
60 MPa
(EXTENSION)
(COMPRESSION)
4
6
8
DEPTH OF EROSION (km)
1.00
0.75
0.50
0.25
$\Delta\sigma_R$
f = 0.0

Figure 14b.

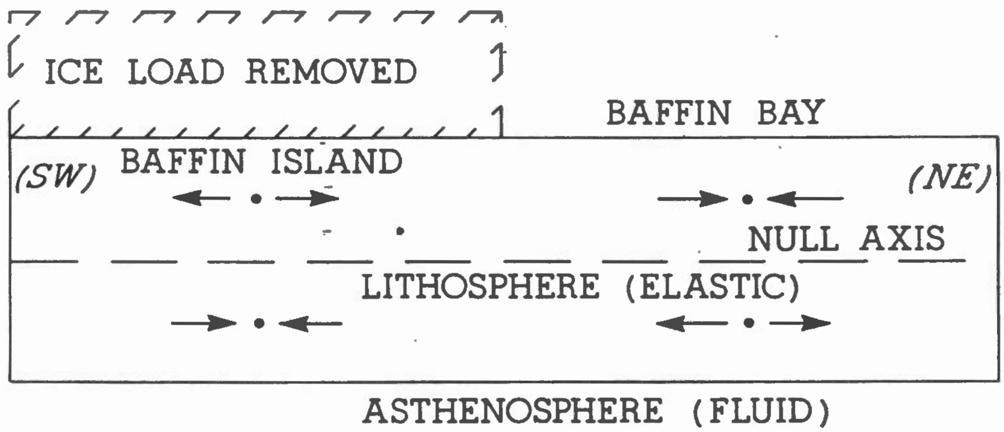
ICE LOAD REMOVED
BAFFIN BAY
(SW)
BAFFIN ISLAND
(NE)
NULL AXIS
LITHOSPHERE (ELASTIC)
ASTHENOSPHERE (FLUID)

Figure 15.

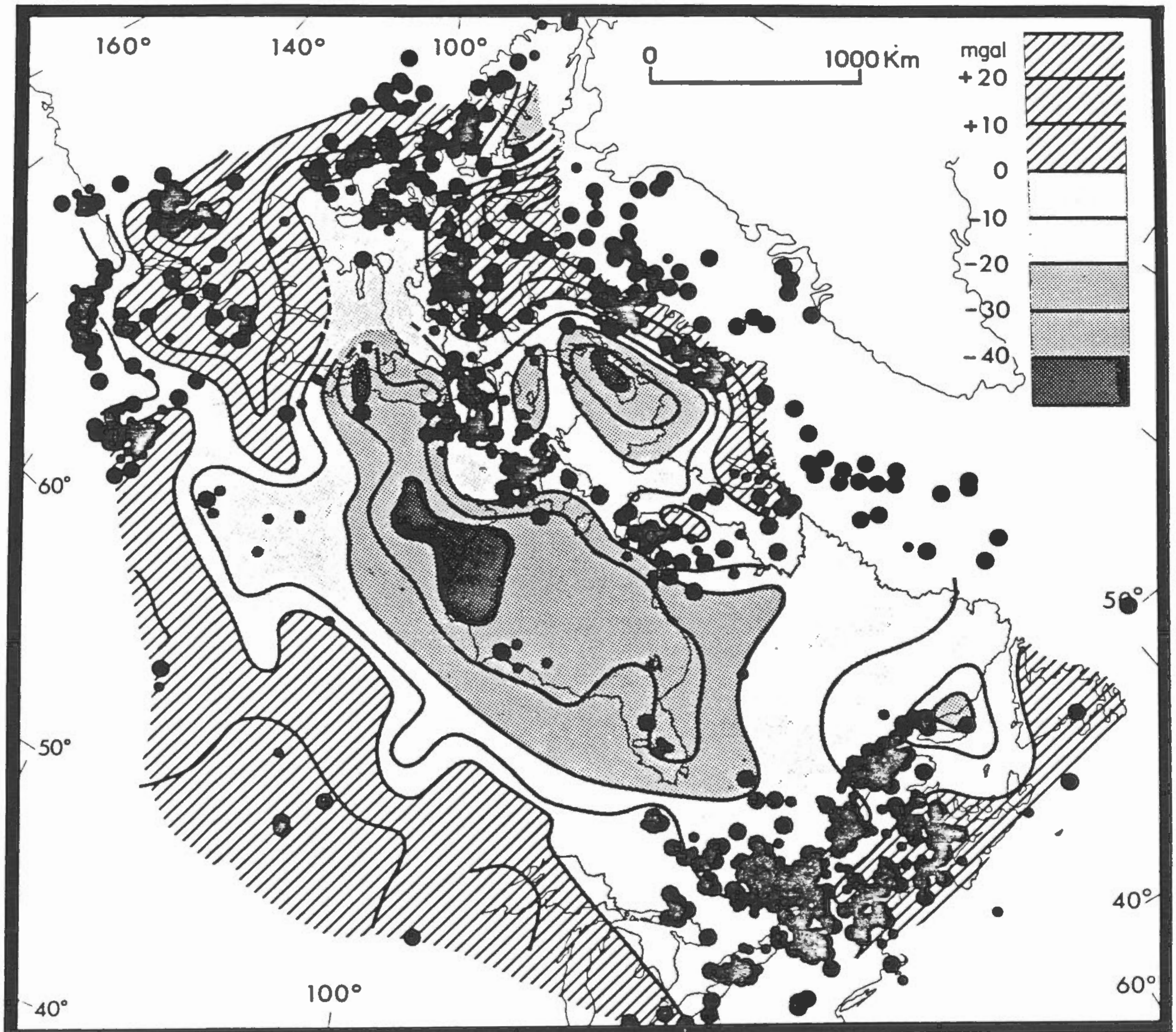

Figure 16.

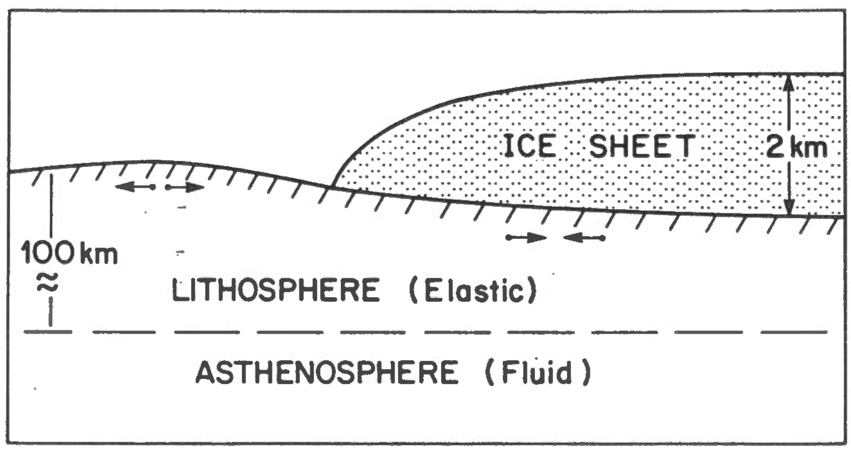
ICE SHEET
2 km
100 km
≈
LITHOSPHERE (Elastic)
ASTHENOSPHERE (Fluid)

Figure 17.

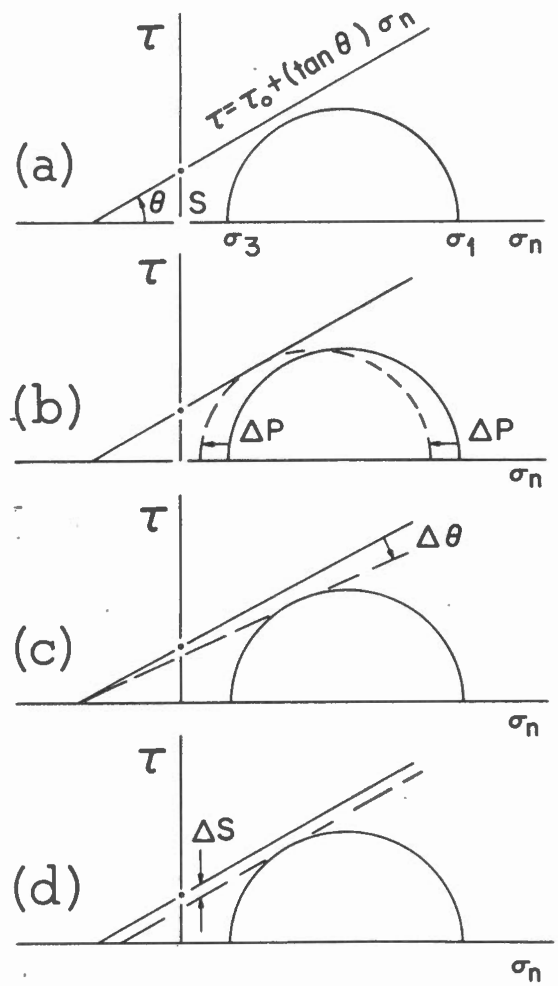

τ
$\tau = \tau_o + (\tan\theta)\,\sigma_n$
(a)
θ
S
σ_3
σ_1
σ_n
τ
(b)
ΔP
ΔP
σ_n
τ
$\Delta\theta$
(c)
σ_n
τ
ΔS
(d)
σ_n

Figure 18.

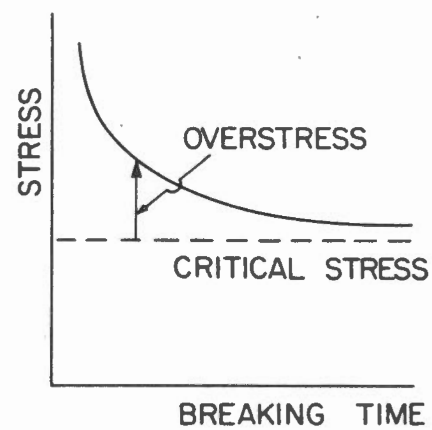

Figure 19.